

Acyl Radical Chemistry via Visible-Light Photoredox Catalysis

Arghya Banerjee^{†a}

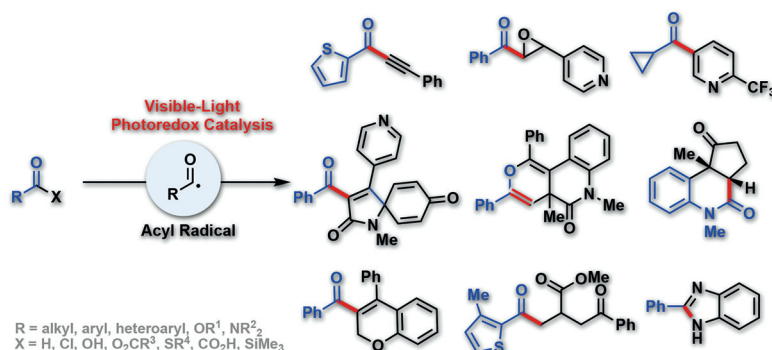
Zhen Lei^{†a}

Ming-Yu Ngai^{*a,b}

^a Department of Chemistry, Stony Brook University, Stony Brook, New York, 11794-3400, USA

^b Institute of Chemical Biology and Drug Discovery, Stony Brook University, Stony Brook, New York, 11794-3400, USA

[†] These authors contributed equally to this work.



Received: 31.08.2018

Accepted after revision: 19.10.2018

Published online: 12.12.2018

DOI: 10.1055/s-0037-1610329; Art ID: ss-2018-e0584-r

Abstract Visible-light photoredox catalysis enables easy access to acyl radicals under mild reaction conditions. Reactive acyl radicals, generated from various acyl precursors such as aldehydes, α -keto acids, carboxylic acids, anhydrides, acyl thioesters, acyl chlorides, or acyl silanes, can undergo a diverse range of synthetically useful transformations, which were previously difficult or inaccessible. This review summarizes the recent progress on visible-light-driven acyl radical generation using transition-metal photoredox catalysts, metallaphotocatalysts, hypervalent iodine catalysts or organic photocatalysts.

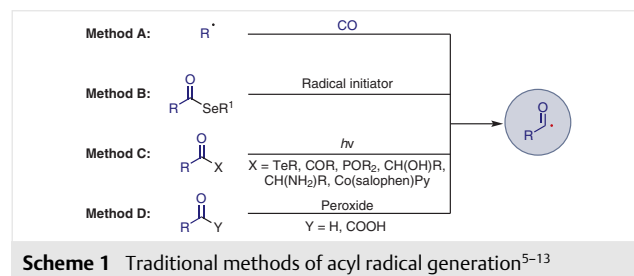
- 1 Introduction
- 2 The Scope of This Review
- 3 Aldehydes as a Source of Acyl Radicals
- 4 α -Keto Acids as a Source of Acyl Radicals
- 5 Carboxylic Acids as a Source of Acyl Radicals
- 6 Anhydrides as a Source of Acyl Radicals
- 7 Acyl Thioesters as a Source of Acyl Radicals
- 8 Acyl Chlorides as a Source of Acyl Radicals
- 9 Acyl Silanes as a Source of Acyl Radicals
- 10 Conclusions and Future Outlook

Key words acylation, photoredox catalysis, acyl radicals, visible light, single-electron transfer, oxidation, reduction, cross-coupling

1 Introduction

Acyl radicals are nucleophilic in nature¹ and serve as versatile synthetic intermediates in Giese-type additions to activated alkenes,² Minisci-type acylations of heteroarenes,³ and for the preparation of a wide range of natural and biologically active molecules.⁴ Conventional approaches to the generation of acyl radicals, however, generally require harsh reaction conditions such as UV irradiation or high temperatures.⁵ One way to access these intermediates is by generation of alkyl radicals from alkyl iodides through photochemical or thermal initiation and

subsequent carbonylation by CO (Scheme 1, method A). The use of acyl selenides in the presence of an organotin reagent such as Bu_3SnH together with a radical initiator^{4a,b} is an alternative means of generating acyl radicals (method B). Through the photochemical cleavage of the $\text{RC}(\text{O})\text{-X}$ bond of acyl tellurides ($\text{X} = \text{Te-R}'$),⁷ benzoylphosphine oxides [$\text{X} = \text{P}(\text{O})\text{Ph}_2$]⁸ can also afford acyl radicals. α -Hydroxy or α -amino ketones $\text{RC}(\text{O})\text{-X}$ [$\text{X} = \text{CH}(\text{OH})\text{R}$ or $\text{CH}(\text{NH}_2)\text{R}$],^{8a,b,9} cyclic ketones (via a Norrish type I cleavage),¹⁰ esters (via photo-Fries rearrangements),¹¹ or acylcobalt salophen reagents [$\text{X} = \text{Co}(\text{salophen})\text{Py}$]¹² can all also deliver acyl radicals (method C). In addition, peroxide-mediated homolytic abstraction of a hydrogen atom from aldehydes and α -keto acids is a viable option for the generation of an acyl radical¹³ (method D). Many directed or non-directed C–H acylation processes catalyzed by transition metals have been developed in the last decades using this strategy.¹⁴ However, from a synthetic viewpoint, their utility was somewhat limited due to the requirement of high energy conditions such as high temperatures, UV irradiation, or stoichiometric amounts of toxic reagents or oxidants.



Scheme 1 Traditional methods of acyl radical generation^{5–13}

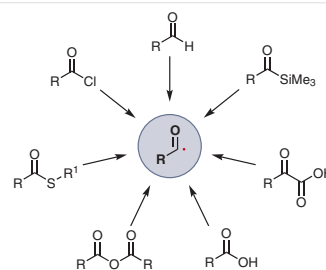
Recently, visible-light photoredox catalysis has emerged as a powerful tool for the synthesis of organic scaffolds that are difficult to prepare by traditional methods.¹⁵ Upon excitation with visible light, photoredox catalysts (PC) generate

an excited photocatalyst (*PC) which can act by single-electron transfer (SET) processes, not only as a one-electron oxidant or a one-electron reductant but also as an energy donor, activating acceptor molecules by an energy-transfer (EnT) process.¹⁶ This photoredox strategy, therefore, provides a new platform for radical reactions by obviating the need for radical initiators and a stoichiometric amount of strong reducing agents. All these features make photoredox catalysis a sustainable alternative from the viewpoint of radical reactions and one that can be utilized as an elegant method to access acyl radicals.

2 The Scope of This Review

Over the past decade, various research groups have reported the visible-light-mediated generation of acyl radicals using photoredox catalysts, metallaphotocatalysts, hypervalent iodine photocatalysts, or organic photocatalysts. This review aims to provide an overview of recent progress

in such visible-light-driven acyl radical generation using aldehydes, α -ketocarboxylic acids, carboxylic acids, carboxylic acid anhydrides, acyl thioesters, acid chlorides, or acyl silanes as acyl radical precursors (Scheme 2). The scope, limitations, and the proposed reaction mechanism of each transformation are discussed. It is noteworthy that most of the reactions described in this review proceed through photoredox catalytic cycles, but the radical chain mechanism cannot be excluded.



Scheme 2 Various modes of acyl radical generation by visible-light photocatalysis

Biographical Sketches



Arghya Banerjee was born in West Bengal, India. He obtained his B.Sc. degree in chemistry from Ramakrishna Mission Vidyamandira, Belur in 2008. After completing his M.Sc. at IIT Gu-

wahati, India in 2010, he undertook his Ph.D. at the same institute under the guidance of Prof. Bhisma K. Patel. In 2017, he joined Stony Brook University as a postdoctoral associate

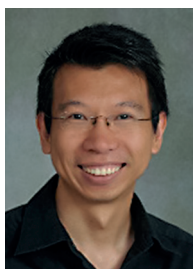
under the supervision of Prof. Ming-Yu Ngai. His current research is focused on the development of novel acylation strategies using photoredox catalysis.



Zhen Lei was born in Xi'an, China. In 2011, he graduated with a B.Sc. degree in chemistry from Sichuan University, China. He continued his studies at the State University of New York at Binghamton, where he worked

with Prof. Susan L. Bane on borazine-containing bioorthogonal reactions and was awarded his M.Sc. degree in 2015. In the same year, he began his Ph.D. studies at Stony Brook University under the guidance of Prof.

Ming-Yu Ngai. His current research focuses on the development of photoredox-catalyzed C–H functionalization and asymmetric reactions.



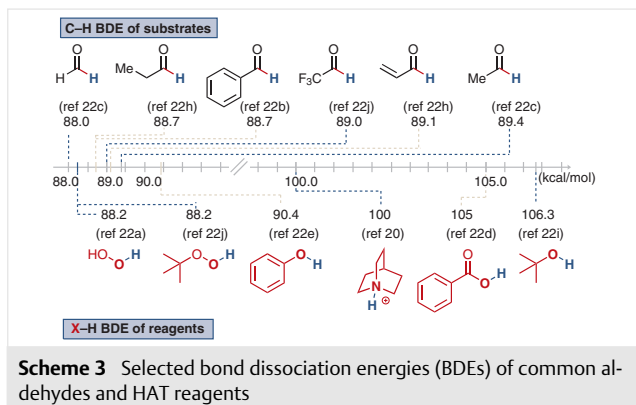
Ming-Yu Ngai was born in Fuching, China and graduated with a B.Sc. degree from the University of Hong Kong in 2003. After receiving his Ph.D. degree with honors in chemistry from the University of Texas at Austin under the guidance of

Prof. Michael J. Krische in 2008, he worked with Prof. Barry M. Trost at Stanford University as a Croucher postdoctoral fellow (2009–2011) and then with Prof. Tobias Ritter at Harvard University as a postdoctoral associate (2011–2013). In 2013,

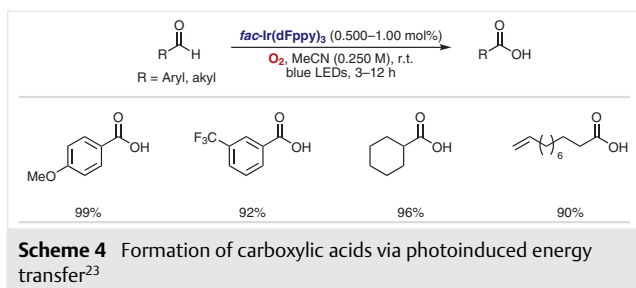
he was appointed as an assistant professor at the Department of Chemistry at Stony Brook University. His research focuses on the development of photoredox catalysis and fluorine chemistry.

3 Aldehydes as a Source of Acyl Radicals

Aldehydes are abundant, readily available, and versatile intermediates that are commonly converted into acyl radicals through hydrogen atom transfer (HAT). In this process, a radical species generated from a HAT reagent abstracts the hydrogen atom of aldehydes forming an acyl radical. Common HAT reagents^{4b,17} such as persulfates¹⁸ and *tert*-butyl hydroperoxide,¹⁹ which are used in traditional thermal radical chemistry, are also applicable to photoredox catalysis. Compounds such as quinuclidine²⁰ and Eosin Y²¹ have also emerged as new HAT reagents for activation of aldehydes. The bond dissociation energies (BDEs) of the C–H of different aldehydes are strikingly similar within 88.0 kcal/mol to 89.4 kcal/mol, while the BDEs of common HAT reagents can range from 88.2 kcal/mol to 106.3 kcal/mol (Scheme 3).^{20,22}

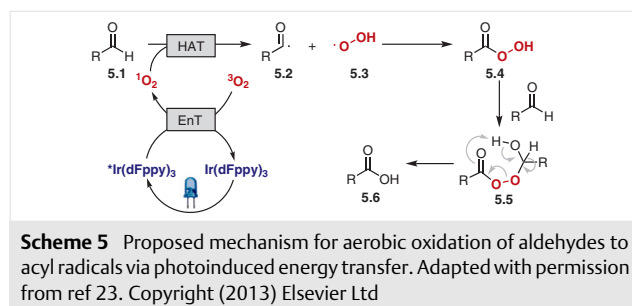


In 2013, Cho et al. reported a synthesis of carboxylic acids through photocatalytic oxidation of aldehydes using molecular O₂ as an oxidant and a HAT reagent (Scheme 4).²³ Both electron-deficient and electron-rich aromatic aldehydes, as well as aliphatic aldehydes, were oxidized to carboxylic acids in excellent yields (90–99%).

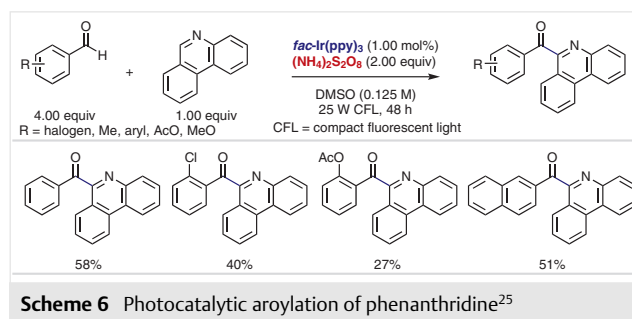


It was proposed that the excited ^{*}Ir(dFppy)₃ ($E^T = 60.1$ kcal/mol)²⁴ ($E^T =$ triplet state energy of the excited photocatalyst) converts triplet ³O₂ into singlet ¹O₂ via photoinduced energy transfer. Singlet ¹O₂ then serves as a HAT re-

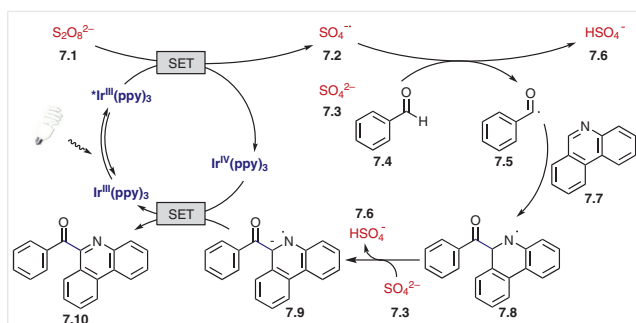
agent that abstracts an aldehyde hydrogen atom to form an acyl radical **5.2** and a hydroperoxyl radical (**5.3**). These two radicals recombine to give a peroxy acid **5.4**, which reacts with another molecule of the aldehyde to afford an adduct **5.5**. This compound then undergoes a Baeyer–Villiger-type rearrangement to form the desired carboxylic acid product **5.6** (Scheme 5).



In 2014, Zeng et al. published a photoredox catalysis method to generate benzoyl radicals from benzaldehydes for the acylation of phenanthridine (Scheme 6).²⁵ Although various benzaldehydes with halogen, alkyl, methoxy, and acetoxy substituents could serve as benzoyl radical donors, phenanthridine was the only radical acceptor reported in this work. The reaction afforded the desired products in yields ranging from 27–73%, but aldehydes with strong electron-donating groups such as *p*-NMe₂ or strong electron-withdrawing groups such as *p*-NO₂ failed to afford the desired products.

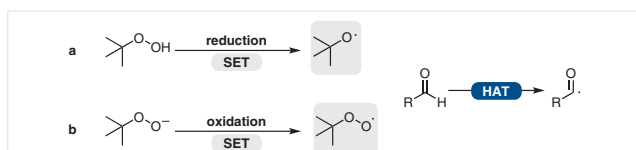


The proposed mechanism of this reaction is shown in Scheme 7. The persulfate salt **7.1** ($E_{1/2}^{\text{red}} = +0.35$ V vs SCE)²⁶ oxidizes the excited *fac*-^{*}Ir(ppy)₃ ($E_{1/2}^{\text{IV/III}} = -1.73$ V vs SCE) via single-electron transfer (SET) to form a sulfate ion **7.3** and a sulfate radical anion **7.2**. The resulting sulfate radical anion abstracts a benzaldehyde hydrogen atom via a HAT process to give the benzoyl radical **7.5**. Subsequent addition of the benzoyl radical to phenanthridine generates an amidyl radical **7.8**, which is deprotonated by SO₄²⁻ to afford a radical anion **7.9**. This radical anion is then oxidized by the Ir^{IV}(ppy)₃ to form the final product **7.10**.



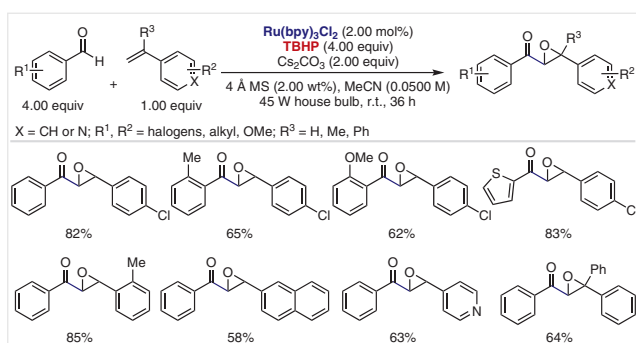
Scheme 7 A persulfate salt as the HAT reagent under photocatalytic conditions. Adapted with permission from ref 25. Copyright (2014) Elsevier Ltd

t-Butyl hydroperoxide (TBHP) is a versatile HAT reagent. While single-electron reduction of TBHP generates the *t*-butoxy radical, single-electron oxidation of deprotonated TBHP affords the *t*-butyl peroxy radical (Scheme 8). Both of these radical species efficiently abstract an aldehyde hydrogen atom, giving an acyl radical.²⁷ Consequently, combining TBHP with photoredox catalysis provides a useful and mild tool for the formation of acyl radicals from aldehydes.



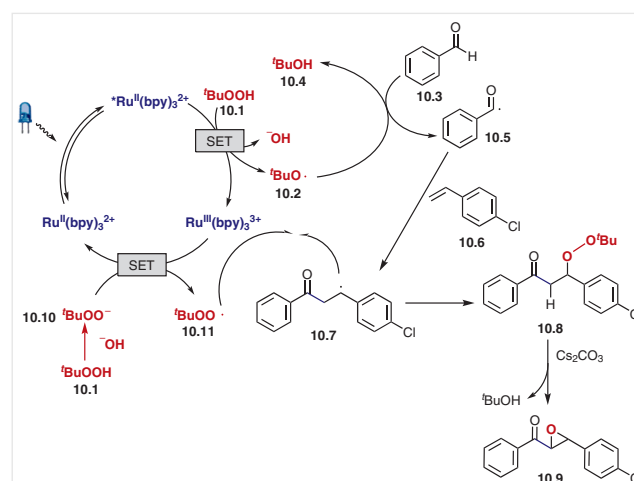
Scheme 8 Abstraction of an aldehyde hydrogen using TBHP

In 2015, Wang and Li reported a synthesis of α,β -epoxy ketones from styrenes and benzaldehydes under photocatalytic conditions using TBHP as a HAT reagent.²⁸ Aromatic aldehydes with halogen, alkyl, and methoxy substituents and thiophenecarboxaldehyde reacted well, giving 61–83% yields (Scheme 9). In terms of the styrene scope, arenes with halogen, alkyl, and methoxy substituents, pyridine, naphthalene, and 1,1-disubstituted styrenes including 1,1-diphenylethylene and α -methylstyrene underwent coupling to afford the desired products in 51–85% yields.



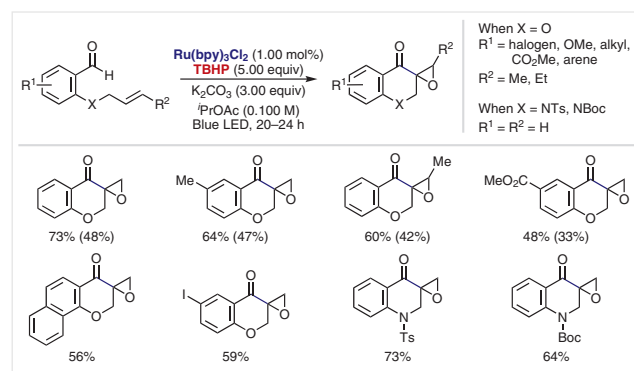
Scheme 9 Photocatalytic synthesis of α,β -epoxy ketones via acyl radical addition using TBHP²⁸

Wang and Li proposed that the *t*-butyl hydroperoxide serves two roles in the reaction. First, TBHP oxidizes the excited $^*Ru^{II}$ ($E_{1/2}^{III/II} = -0.81$ V vs SCE) to form a hydroxide and a *t*-butoxy radical $^tBuO\cdot$, which subsequently abstracts a hydrogen atom from the aldehyde to give a benzoyl radical. Second, deprotonation of the TBHP by the hydroxide ion ^-OH gives a *t*-butyl peroxy anion $^tBuOO^-$, which reduces the oxidized $Ru^{III}(bpy)_3^{2+}$ regenerating the photocatalyst and forming a *t*-butyl peroxy radical $^tBuOO\cdot$. Recombination of the *t*-butyl peroxy radical with the radical intermediate **10.7** affords a β -peroxy ketone **10.8**, which undergoes base-promoted elimination of $^tBuO^-$ to produce the final product **10.9** (Scheme 10).



Scheme 10 Proposed mechanism for the photocatalytic synthesis of α,β -epoxy ketones via an acyl radical intermediate. Adapted with permission from ref 28. [Copyright (2015) American Chemical Society]

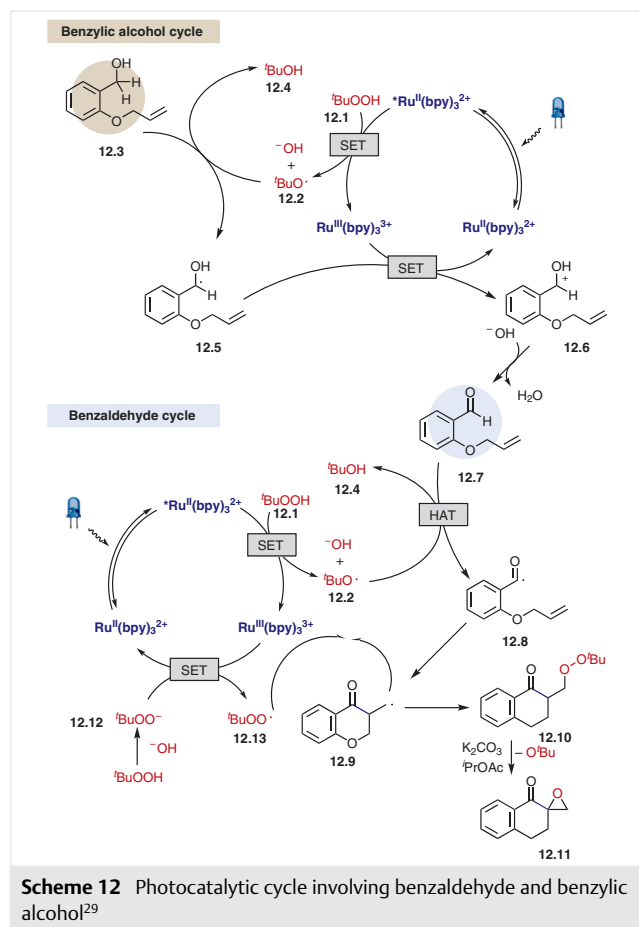
In 2017, Hong et al. reported an intramolecular cyclization and epoxidation (Scheme 11), developed in analogy to the intermolecular method reported by Wang and Li,²⁸ using TBHP as the HAT reagent.²⁹ The reaction conditions were applicable to both allyloxy and allylamino substrates



Scheme 11 Intramolecular acyl radical addition/epoxidation.²⁹ The yields in parentheses were obtained by the reaction of benzyl alcohol substrates using 8 equivalents of TBHP

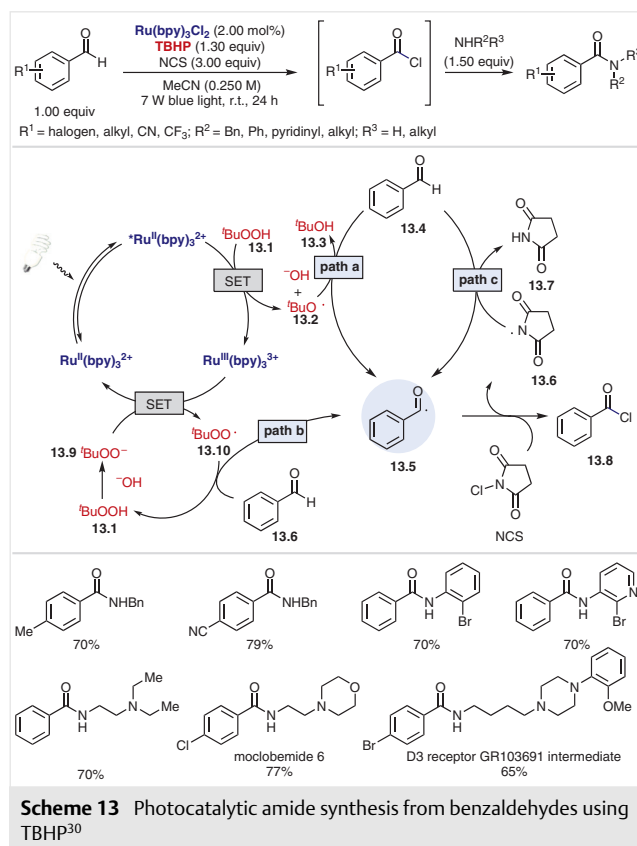
to produce the desired spiroepoxy chroman-4-ones and enamines. Interestingly, a three-step tandem process starting from benzyl alcohol and using 8 equivalents of TBHP also occurred, albeit with lower yields being obtained.

It was reported that addition of TEMPO completely inhibits the reaction and forms the TEMPO adduct, which indicates the involvement of a radical intermediate. Exposure of the β -peroxy ketone **12.10** to a solution of K_2CO_3 in $iPrOAc$ afforded the desired α -carbonyl epoxide **12.11**, suggesting that the product is derived from the β -peroxy ketone intermediate. Based on these experimental results and the observation that benzylic alcohols also afforded the desired spiroepoxy chroman-4-ones, tandem oxidation of the benzylic alcohols to aldehydes followed by radical cyclization was proposed (Scheme 12). TBHP (**12.1**) oxidatively quenches the excited $*Ru^{II}(bpy)_3^{2+}$ to generate $Ru^{III}(bpy)_3^{3+}$ and a *t*-butoxy radical ($^tBuO^{\cdot}$) (**12.2**). This radical abstracts an α -hydrogen atom from the benzylic alcohol **12.3** to generate an α -hydroxy radical **12.5**, which is oxidized and deprotonated to form benzaldehyde **12.7**. Once the benzaldehyde is formed, the rest of the reaction mechanism is parallel to the catalytic cycle proposed by Wang and Li.²⁸

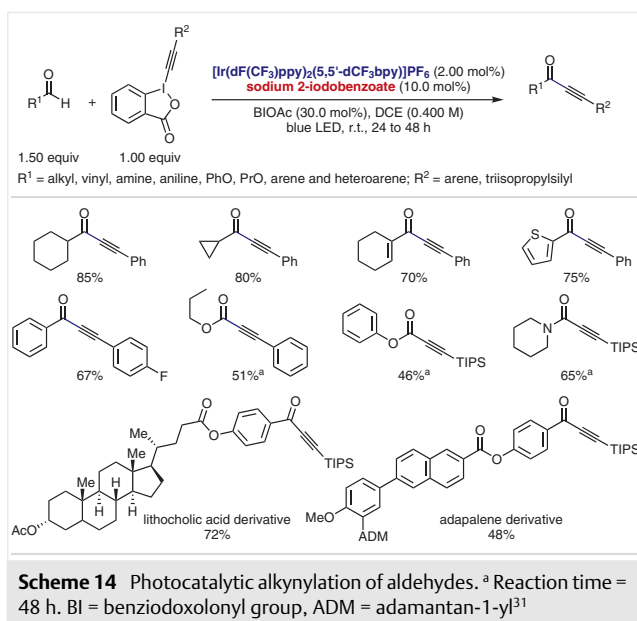


Following Wang's discovery using TBHP for the generation of acyl radicals, Cho and Iqbal, in 2016, disclosed a photocatalytic amide formation protocol from aldehydes and amines (Scheme 13).³⁰ It was proposed that reduction of TBHP affords hydroxide and the *t*-butoxy radical, which undergoes HAT with benzaldehyde to form the benzoyl radical **13.5** (path a). This radical abstracts the chlorine atom from *N*-chlorosuccinimide, forming benzoyl chloride **13.8**, which reacts with an amine to afford the amide product. The reaction proceeds with a sub-stoichiometric quantity of TBHP, leading to speculation that other radical species such as the *t*-butyl peroxy radical (path b) and the succinimide radical (path c) generated in the reaction mixture might also be responsible for the HAT of benzaldehyde leading to the benzoyl radical.

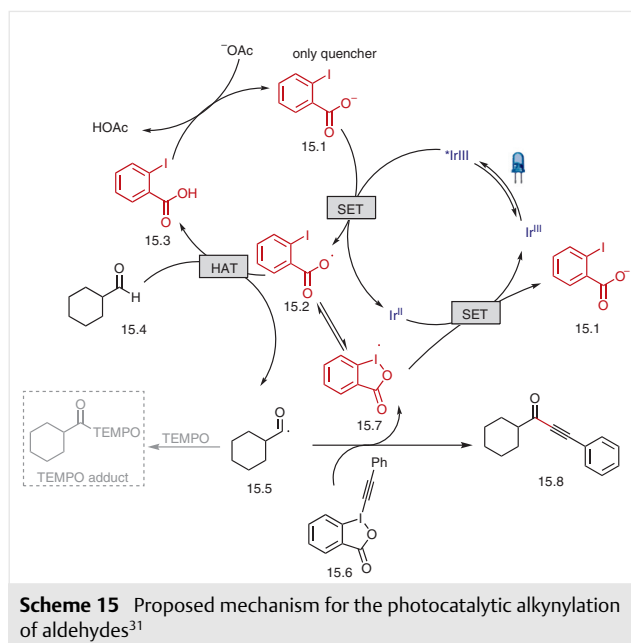
This reaction has a broad substrate scope. Both electron-rich and electron-poor benzaldehydes with substituents such as alkyl, halogens, cyano, and CF_3 underwent coupling to afford the desired amides in 65–87% yields. Primary and secondary amines, anilines, and aminopyridines were all viable substrates giving the desired products in 58–82% yields. This strategy was used in the synthesis of the antidepressant moclobemide **6** and the D3 receptor GR103691 intermediate (Scheme 13).



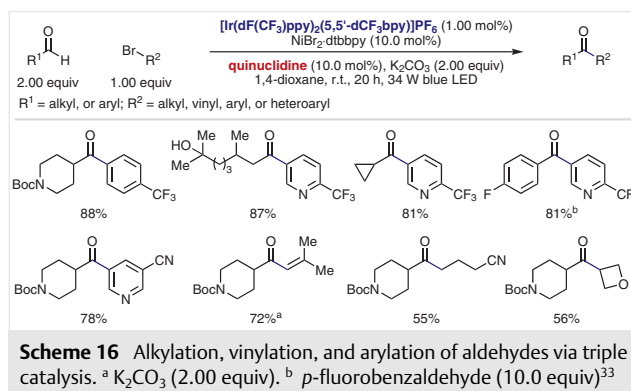
In 2017, Glorius et al. reported a photocatalytic alkylation of aldehydes, formates, and formamides using alkynylbenziodoxolones as the alkyne source and the resulting benziodoxolonyl radical as a HAT reagent.³¹ This reaction has a broad substrate scope and a wide range of alkyl, vinyl, aryl, and heteroaryl aldehydes, formates, and formamides reacted with various aryl or silyl alkynylbenziodoxolones to afford the desired alkynylated products in 46–90% yields (Scheme 14). The carbonyl radicals generated under the optimized conditions failed to react with double bonds, and thus the method is compatible with α,β -unsaturated aldehydes. This transformation is also compatible with late-stage alkylation of complex substrates such as cholesterol, lithocholic acid, probenecid, and adapalene derivatives, giving the desired products in 48–78% yields.



Stern–Volmer quenching experiments showed that the 2-iodobenzoate was the only component that quenched the photocatalyst. In the presence of TEMPO, the formation of the alkynylated product was completely inhibited, and a TEMPO-trapped adduct was obtained. On the basis of these results, the authors proposed that 2-iodobenzoate (**15.1**) reductively quenches the excited [$^*Ir(dF(CF_3)ppy)_2(5,5'-dCF_3bpy)]PF_6$ ($E_{1/2}^{III^*/II} = +1.21$ V vs SCE)³² to form Ir^{II} and the 2-iodobenzoyloxy radical **15.2** (Scheme 15). Hydrogen-atom abstraction of the aldehyde hydrogen by **15.2** provides a carbonyl radical **15.5** that reacts with alkynylbenziodoxolone **15.6** to form the desired product **15.8**, simultaneously releasing the benziodoxolonyl radical **15.7**. Reduction of **15.7** with Ir^{II} forms **15.1** and regenerates the ground state Ir photocatalyst. Alternatively, since **15.7** is in equilibrium with **15.2**, it can undergo a HAT reaction directly.

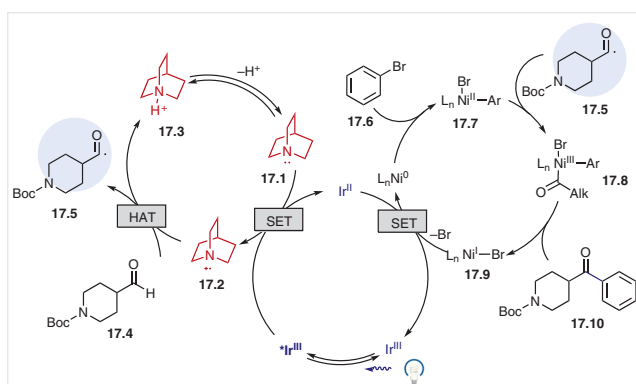


In 2017, MacMillan et al. reported a triple catalytic protocol for arylation, vinylation, and alkylation of aldehydes via an acyl radical intermediate using aryl, vinyl, and alkyl bromides as coupling partners and quinuclidine, Ni^{II} , and a photocatalyst as catalysts (Scheme 16).³³ This approach has a very broad scope and is insensitive to the electronic nature of the aryl bromides. Heteroaryl, cyclic and acyclic vinyl, and alkyl bromides are viable substrates and afforded the desired ketones in 50–90% yields. Regarding the aldehyde scope, both alkyl and aryl aldehydes coupled well to afford the desired products in 70–90% yields, although 6–10 equivalents of aryl aldehydes were needed.



The mechanistic hypothesis for this triple catalysis is shown in Scheme 17. SET from quinuclidine ($E_{1/2}^{ox} = +1.10$ V vs SCE in MeCN)²⁰ to the excited [$^*Ir(dF(CF_3)ppy)_2(5,5'-dCF_3bpy)]PF_6$ ($E_{1/2}^{III^*/II} = +1.21$ V vs SCE) generates an electrophilic quinuclidinium cation radical **17.2**, which selectively abstracts the weak and hydridic aldehyde hydrogen

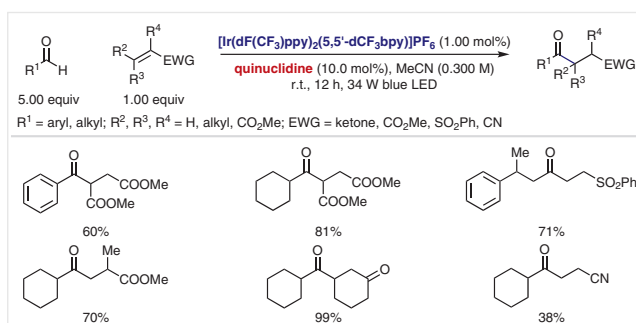
atom to form the acyl radical **17.5**. The α -amino C–H bond also exhibits hydric bond polarization and is subjected to hydrogen atom abstraction.³⁴ The authors discovered that the reaction performed in 1,4-dioxane circumvented the unwanted competing α -amino C–H activation affording exclusively the desired acylated product, whereas MeCN or DMSO solvents delivered the α -amino arylation product in addition to the desired product. Oxidative addition of the aryl bromide to Ni⁰ on the other hand delivers an aryl–Ni^{II} species **17.7**, which is intercepted by the acyl radical **17.5** to form acyl–Ni^{III} complex **17.8**. Subsequently, reductive elimination forms the desired ketone product and a Ni^I species **17.9**. A single-electron transfer between Ir^{II} and Ni^I regenerates the Ir^{III} and Ni⁰ catalysts and completes the catalytic cycle.



Scheme 17 Proposed reaction mechanism for the triple catalysis. Adapted with permission from ref 33. Copyright (2017) American Chemical Society

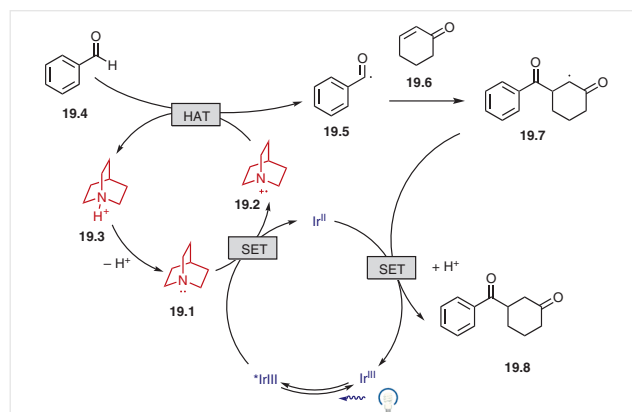
Also in 2017, Liu et al. used the quinuclidine catalyst to generate the acyl radical from aldehydes under photoredox conditions (Scheme 18).³⁵ Both aromatic and aliphatic aldehydes were viable substrates under the dual-catalytic conditions. The synthetic utility was also well demonstrated by a variety of electron-deficient olefin acceptors.

With a mechanism similar to that described in Scheme 17, reductive quenching of the excited ^{*}Ir^{III} catalyst by quinuclidine (**19.1**) forms a HAT reagent **19.2**, which abstracts



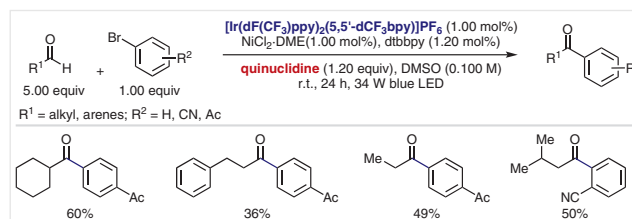
Scheme 18 Photocatalytic hydroacylation using quinuclidine as the HAT reagent³⁵

the aldehyde hydric hydrogen to form an acyl radical. The acyl radical is then intercepted by an olefin to give the carbon radical intermediate **19.7**. A single-electron transfer from Ir^{II} to this intermediate, followed by protonation, delivers the desired product and regenerates the Ir^{III} catalyst (Scheme 19).



Scheme 19 Photocatalytic hydroacylation of alkenes promoted by quinuclidine³⁵

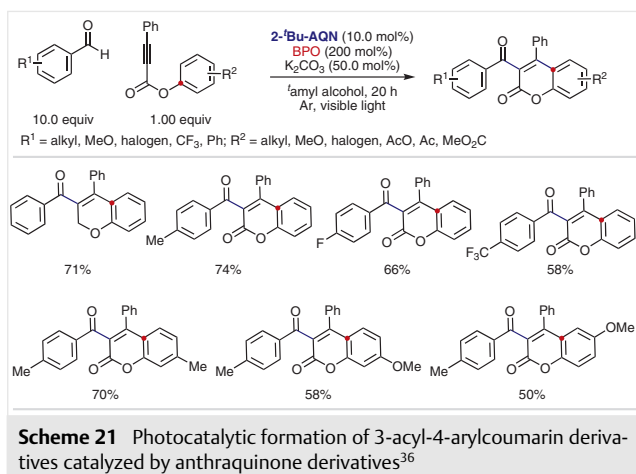
In the same paper,³⁵ Liu et al. presented their preliminary results of a catalytic cross-coupling process using the Ir photocatalyst and NiCl₂. In contrast to MacMillan's work,³³ Liu et al. used a stoichiometric amount of quinuclidine, and the scope of the reaction was significantly limited as a result of the unwanted reduction of aryl bromides (Scheme 20).



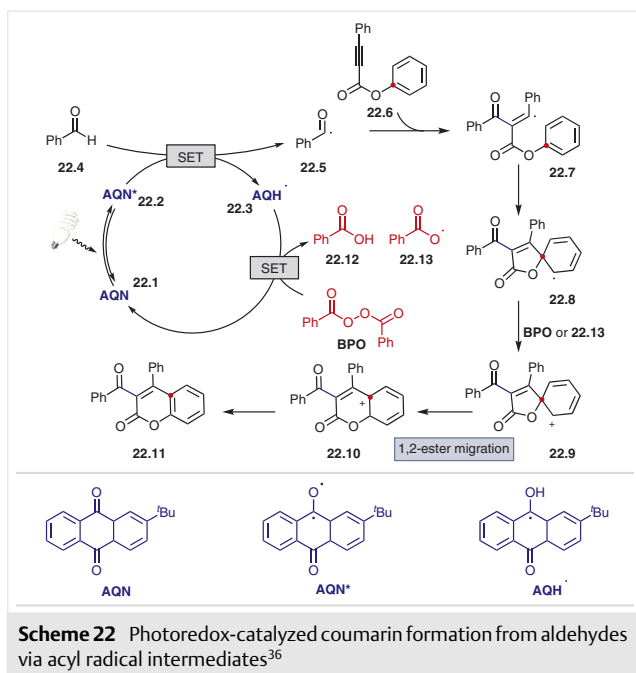
Scheme 20 Preliminary results of metallophotocatalytic cross-coupling using NiCl₂³⁵

In 2018, Itoh et al. used 2-*t*-butylantraquinone (2-*t*-Bu-AQN) as a photocatalyst and benzoyl peroxide (BPO) as an oxidant in the presence of potassium carbonate to synthesize 3-acyl-4-aryl coumarin derivatives (Scheme 21).³⁶ Alkyl, alkoxy, and acetoxy groups on both the benzaldehyde and propynate substrates were well tolerated. The authors showed that many of their coumarin products had potential biological applications as demonstrated by their effectiveness in the inhibition of PSA secretion and the proliferation of androgen-dependent prostate cancer.

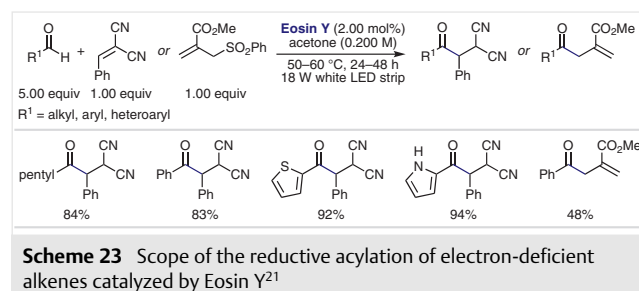
The proposed mechanism for this reaction is depicted in Scheme 22. Photoexcited 2-*t*-butylantraquinone **22.2** acts as a HAT reagent and abstracts the formyl hydrogen atom of



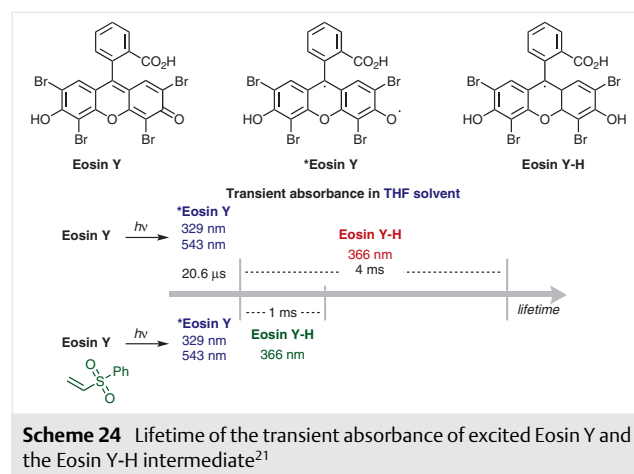
benzaldehyde, forming the semiquinone radical³⁷ AQH[•] (**22.3**) and the benzoyl radical **22.5**. Addition of the benzoyl radical to the propynate **22.6** generates a vinyl radical intermediate **22.7**, which undergoes 5-*exo-trig* cyclization to afford a spirocyclic species **22.8**. This spirocyclic intermediate is then oxidized by either BPO or the benzoyloxyl radical **22.13** to form a carbocation **22.9**. 1,2-Ester migration and deprotonation afforded the desired product **22.11**. Oxidation of AQH[•] by BPO, followed by deprotonation produced benzoic acid, the benzoyloxyl radical and the ground state AQN catalyst. This reaction also proceeds under thermal conditions, where a 54% yield was obtained in the absence of the photocatalyst, indicating that the benzoyloxy radical formed from the thermal decomposition of benzoyl peroxide can also function as an alternative HAT reagent.



In 2018, Wu et al. reported that excited Eosin Y, functioning as a HAT reagent, can abstract the aldehyde hydrogen atom under irradiation with an 18 W white LED light (Scheme 23).²¹ Alkyl, aryl and heteroaryl aldehydes reacted with electron-deficient 1,1-dicyano-2-phenylethylene to afford the desired products in 83–94% yields. Benzaldehyde can react with a SOMophile such as methyl 2-[(phenylsulfonyl)methyl]acrylate to form an allylation product in 48% yield. It should be noted that the major focus of Wu's work was on the alkylation of a wide range of C–H bonds with electron-deficient alkenes under photocatalytic conditions. The C–H partners include THF, thioethers, amides, alcohols, and cyclohexane. However, these coupling reactions are outside the scope of this review.

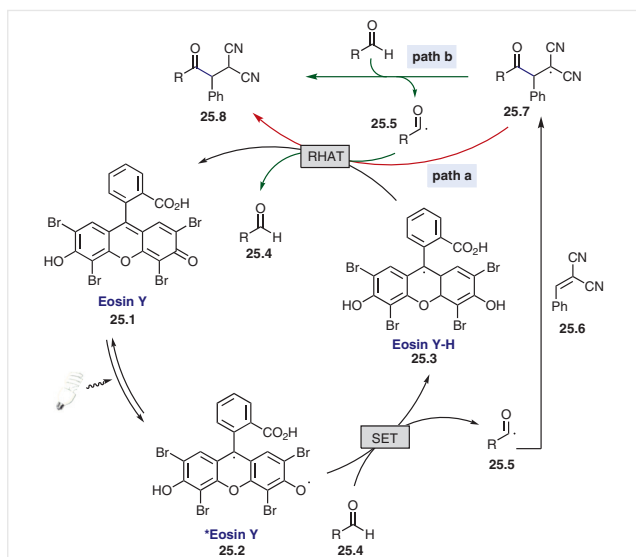


Anionic Eosin Y is commonly engaged in SETs under photoredox-catalyzed conditions. However, neutral Eosin Y, which was used by Wu et al.,²¹ is inactive in SET processes.³⁸ It was shown that neither THF nor phenyl vinyl sulfone quenches the excited Eosin Y indicating that the reaction did not proceed through single-electron transfer or energy transfer. Transient absorbance experiments showed that the excited *Eosin Y absorbs at both 329 nm and 543 nm, whereas Eosin Y-H absorbs at 366 nm. In the presence of phenyl vinyl sulfone, a radical acceptor, the decay of Eosin Y-H was much faster than took place in the absence of the alkene (Scheme 24), demonstrating the feasibility of HAT



between Eosin Y-H and radical intermediates formed during the coupling process. The quantum yield of the reaction was estimated to be 0.40.

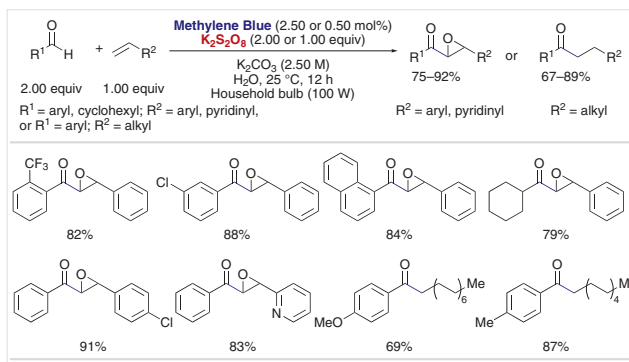
On the basis of these mechanistic studies, Wu et al. proposed the direct photocatalytic hydrogen atom transfer mechanism shown in Scheme 25.^{21,39} Photoexcitation of Eosin Y (**25.1**) affords excited *Eosin Y (**25.2**), which abstracts an aldehyde hydrogen atom to form an acyl radical species **25.5** and Eosin Y-H (**25.3**). The acyl radical is subsequently trapped by an electron-deficient alkene to form the alkyl radical intermediate **25.7**. At this stage, there are two reaction pathways accounting for the formation of the desired product and regeneration of the Eosin Y catalyst. In path a, a reverse hydrogen atom transfer (RHAT) between the Eosin Y-H and radical species **25.7** affords the final product and the Eosin Y catalyst. In path b, aldehyde **25.4** undergoes HAT with the radical species **25.7** to form the desired product **25.8** and an acyl radical **25.5**. The acyl radical reacts with Eosin Y-H via RHAT to afford an aldehyde and regenerate the Eosin Y catalyst. Although the authors performed computational and deuterium labeling studies, they could not distinguish between these two pathways.



Scheme 25 A direct HAT process photocatalyzed by Eosin Y²¹

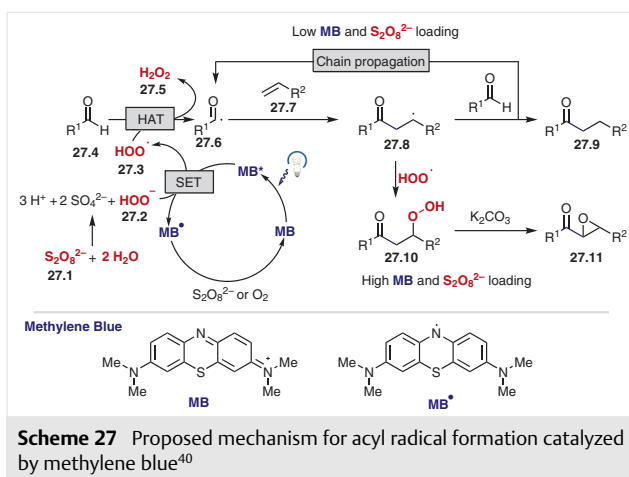
Salles et al., in 2018, achieved acyl-epoxylation and hydroacylation of alkenes using methylene blue (MB) as a photoredox catalyst and $K_2S_2O_8$ as an oxidant in air-equilibrated water solution (Scheme 26).⁴⁰ With high loading of the photocatalyst and oxidant (2.50 mol% and 2.00 equiv, respectively), simple benzaldehydes with the arene moiety substituted with Me, Cl, F, MeO or CF_3 reacted with styrenes or 2-vinylpyridine to afford the desired epoxide products in 75–92% yields. 1-Naphthaldehyde and cyclohexanecarboxaldehyde were also viable substrates forming the final products in 84% and 79% yields. With lower loading of the photocatalyst and oxidant (0.500 mol% and 1.00 equiv, re-

spectively), benzaldehydes coupled with long-chain aliphatic alkenes to deliver the hydroacylated products in 67–89% yields.



Scheme 26 Epoxyacylation and hydroacylation using methylene blue as the photocatalyst and persulfate as the oxidant⁴⁰

The reaction of benzaldehyde and styrene using $K_2S_2O_8$ in the absence of K_2CO_3 only afforded trace acyl-epoxyated product, whereas the reaction proceeded well using H_2O_2 in the presence of K_2CO_3 . Based on these observations and literature precedents,⁴¹ a reaction mechanism involving a hydroperoxide anion as a HAT reagent was proposed and is shown in Scheme 27. Persulfate anion **27.1** reacts with water under basic conditions to generate the hydroperoxide anion **27.2** ($E_{1/2}^{red} = -0.88$ V vs SHE),⁴² which undergoes single-electron oxidation with excited MB^* ($E_{1/2}^{red} = -1.21$ V vs SHE) to form a hydroperoxyl radical (**27.3**) and methylene blue neutral radical MB^{\bullet} . Oxidation of MB^{\bullet} by the $S_2O_8^{2-}$ or O_2 regenerates the methylene blue catalyst. The hydroperoxyl radical abstracts an aldehyde hydrogen atom to form an acyl radical **27.6**, which adds onto an alkene to give the alkyl radical intermediate **27.8**. With the lower loading of the photocatalyst and oxidant, the alkyl radical **27.8** undergoes HAT with an aldehyde substrate to afford the desired hydroacylation product **27.9** via a radical-chain propagation

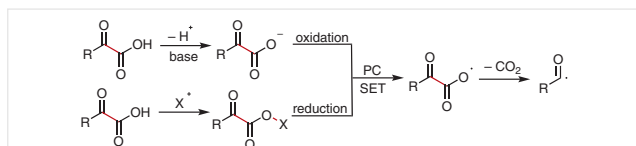


Scheme 27 Proposed mechanism for acyl radical formation catalyzed by methylene blue⁴⁰

tion process. With a higher loading of the photocatalyst and persulfate anion, the alkyl radical **27.8** is trapped by the hydroperoxyl radical to deliver the β -peroxyl adduct **27.10**. Finally, base-promoted elimination affords the desired epoxide product **27.11**.

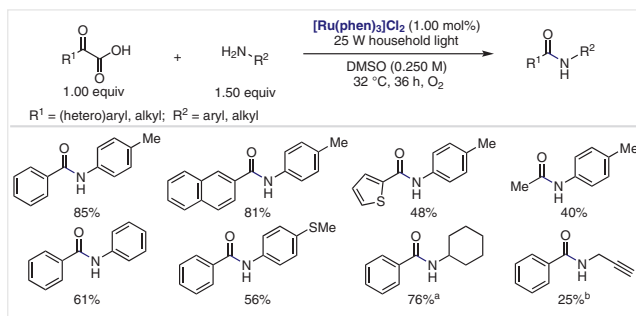
4 α -Keto Acids as a Source of Acyl Radicals

Conversion of α -keto acids into the acyl radical equivalents can be achieved via single-electron transfer of the corresponding carboxylate by photocatalytic oxidation and subsequent decarboxylation. Alternatively, installation of a good leaving group (X), e.g., as in *N*-hydroxyphthalimide, generates a keto ester that can be reduced by a photoredox catalyst (PC) and forms an acyl radical after further decarboxylation (Scheme 28).



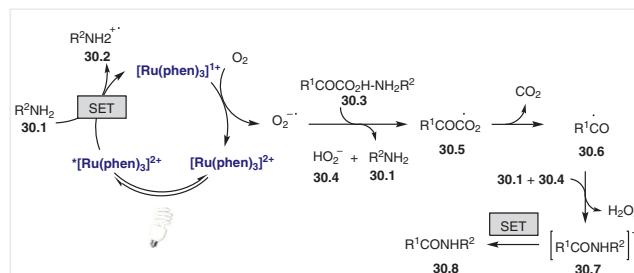
Scheme 28 Generation of an acyl radical from α -keto acids by photoredox catalysis

In 2014, Lei and Lan reported the first visible-light-mediated photocatalytic oxidative decarboxylation of α -keto acids in the synthesis of amides.⁴³ This efficient radical decarboxylative coupling was catalyzed by the photocatalyst $[\text{Ru}(\text{phen})_3]\text{Cl}_2$ ($E_{1/2}^{\text{II}^*/\text{I}}$ = +0.82 V vs SCE)⁴⁴ and molecular oxygen as an oxidant. A wide range of electron-donating and electron-withdrawing aromatic α -keto acids reacted smoothly under these reaction conditions to afford the desired amides in good yields (64–85%) (Scheme 29). Heteroaromatic and aliphatic α -keto acids provided the desired products in 48–79% yields. Various electron-rich aromatic and aliphatic amines gave the corresponding products in 40–79% and 25–77% yields, respectively.



Scheme 29 Visible-light-mediated decarboxylation/oxidative amidation of α -keto acids with amines.⁴³ ^a Using 10 equivalents of amine. ^b Using 5 equivalents of amine

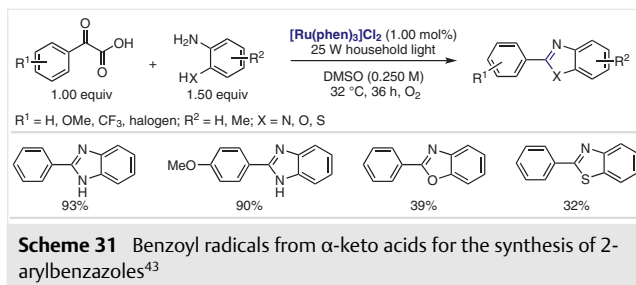
A series of studies was conducted to examine the reaction mechanism. For example, cyclic voltammetry (CV) experiments on an α -keto acid salt (PhCOCO_2K) suggest an oxidative decarboxylation path, TEMPO-trapping experiments confirm the formation of an acyl radical, and DFT calculations support the reaction between acyl radicals and amines followed by deprotonation leading to an amide radical anion. Interestingly, in the absence of the α -ketocarboxylic acid, EPR studies of this photocatalytic reaction detected two peaks: $[\text{Ru}(\text{phen})_3]^+$ and an amine radical. Addition of an α -ketocarboxylic acid diminishes the organic radical peak and only the $[\text{Ru}(\text{phen})_3]^+$ peak remains. Thus, the authors proposed that the oxidation of $[\text{Ru}(\text{phen})_3]^+$ by molecular oxygen is crucial and probably the rate-determining step of this process. Based on these results, a possible reaction mechanism was proposed and is shown in Scheme 30. Reductive quenching of the excited photocatalyst $^*[\text{Ru}(\text{phen})_3]^{2+}$ by an amine forms an amine radical cation **30.2** and $[\text{Ru}(\text{phen})_3]^+$. Single-electron oxidation of $[\text{Ru}(\text{phen})_3]^+$ by molecular oxygen affords the ground state photocatalyst, $[\text{Ru}(\text{phen})_3]\text{Cl}_2$, and a superoxide radical anion, which deprotonates and oxidizes the ammonium α -ketocarboxylate salt **30.3** to produce the dicarbonyl radical intermediate **30.5**. Decarboxylation of **30.5** gives acyl radical **30.6**, which is then trapped by amine **30.1** followed by deprotonation in the presence of a hydrogen peroxide anion HO_2^- (**30.4**) to produce the amide radical anion **30.7**. Oxidation of **30.7** via a SET process affords the desired amide product **30.8**.



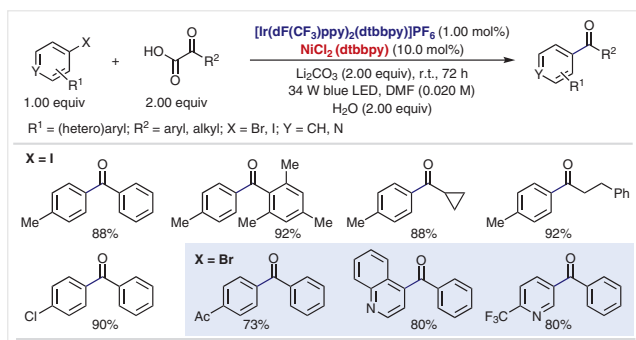
Scheme 30 Mechanism for the amidation from α -keto acids and amines⁴³

This method was also applied to anilines, *o*-substituted with NH_2 , OH , and SH groups, to construct important heterocyclic compounds such as benzimidazoles (68–93%), benzoxazoles (39–46%), and a benzothiazole (32%) in good yields (Scheme 31).

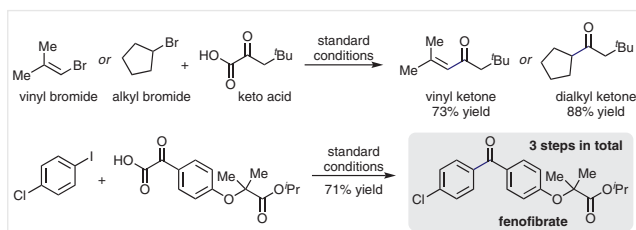
Following initial studies by Lei and Lan on photoredox-catalyzed decarboxylative amidation,⁴³ this acyl radical generation from α -keto acids has been employed in several radical coupling reactions. For example, in 2015, Macmillan et al. reported the first decarboxylative arylation of α -keto acids using aryl halides via a merger of visible-light pho-



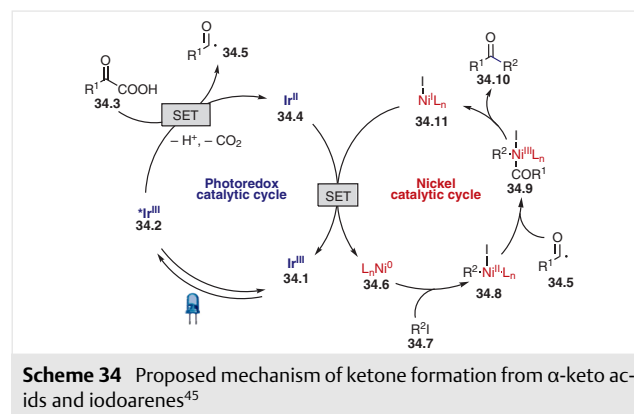
to redox catalysis and nickel catalysis.⁴⁵ Substituted aromatic and aliphatic α -keto acids are compatible under the reaction conditions and provide moderate to excellent yields (57–92%) of the desired ketones (Scheme 32). A sterically hindered *o*-substituted α -keto acid was also efficiently coupled under the same reaction conditions and provided the desired product in high yield (92%). Halo-arenes (halo = Br, I) and halo-heteroarenes containing electron-donating and electron-withdrawing substituents also provided the desired ketones in 70–90% and 64–85% yields, respectively.



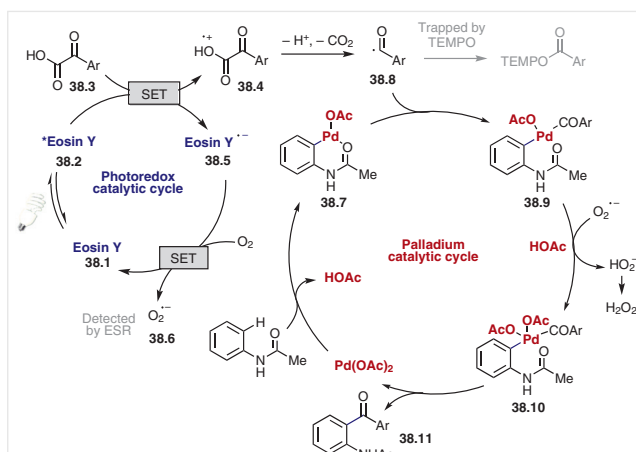
Further generalization of this method was demonstrated by successfully coupling hindered vinyl halides and cyclopentyl bromide with α -keto acids under the optimized reaction conditions to generate a vinyl ketone and a dialkyl ketone in good yields (73–88%). This strategy was also elaborated for the synthesis of fenofibrate, a cholesterol-controlling drug (Scheme 33).



The authors proposed that the strongly oxidizing excited $^*[\text{Ir}(\text{dFCF}_3\text{ppy})_2(\text{dtbbpy})]^+$ (**34.2**) ($E_{1/2}^{\text{III/II}} = +1.21$ V vs SCE in MeCN),⁴⁶ generated upon visible-light irradiation, reacts with the α -ketocarboxylate via single-electron oxidation to generate the corresponding carboxyl radical species and the reduced photocatalyst **34.4**. This carboxyl radical species subsequently delivers the acyl radical species **34.5** via decarboxylation. SET from the strong reducing Ir^{II} species **34.4 ($E_{1/2}^{\text{III/II}} = -1.37$ V vs SCE in MeCN)⁴⁶ to the in situ generated Ni^I-dtbbpy complex would afford the Ni⁰ catalyst **34.6**, which initiates the second catalytic cycle through oxidative addition to the aryl halide to generate the Ni^{II} aryl complex **34.8**. The addition of the nucleophilic acyl radical **34.5** to **34.8** produces the nickel acyl complex **34.9**. Final reductive elimination from this Ni^{III} complex provides the desired ketone **34.10** with the regeneration of the Ni^I-dtbbpy complex **34.11** (Scheme 34).**

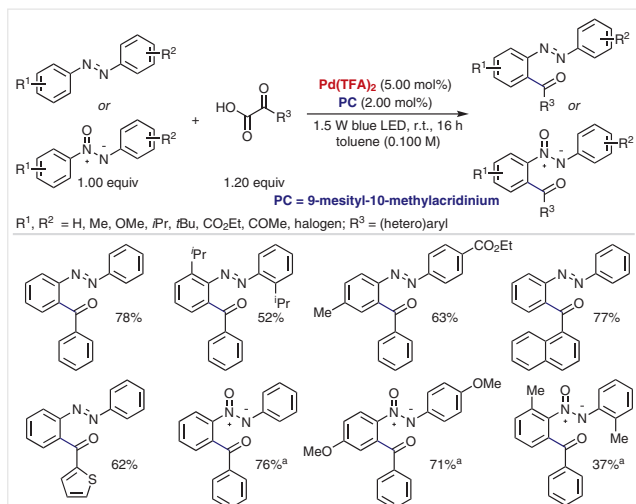


In the last decades, palladium has been widely used in various transition-metal-catalyzed decarboxylative cross-coupling reactions.⁴⁷ A typical example is the decarboxylative acylation of aryl halides using α -keto acids.⁴⁸ In 2015, Shang and Fu combined photoredox and palladium catalysis and achieved such decarboxylative cross-coupling reactions for the first time.⁴⁹ The reported decarboxylative coupling strategy of aryl halides with α -ketocarboxylic acids provides access to various unsymmetrical ketones. The electronic and steric effects of the substituents present in aryl halides have no substantial effects on the yields of the products (74–96%). Interestingly, aryl iodides containing a *t*-butoxycarbonyl (Boc)-protected phenylalanine ester and an aryl boronic pinacol ester both provided the corresponding products in 88% and 70% yields. This reaction is compatible with electron-donating aryl groups (82–95%) as well as heteroaryl (46–89%) and alkyl α -ketocarboxylic acids (60–89%), but the presence of electron-withdrawing substituents on the aryl ring of the α -ketocarboxylic acids sharply decreased the product yield to ~10%. The use of an external phosphine ligand (NiXantphos) in the case of bromoarenes is due to their relatively slow oxidative addition to the Pd⁰ catalyst when compared to iodoarenes (Scheme 35).



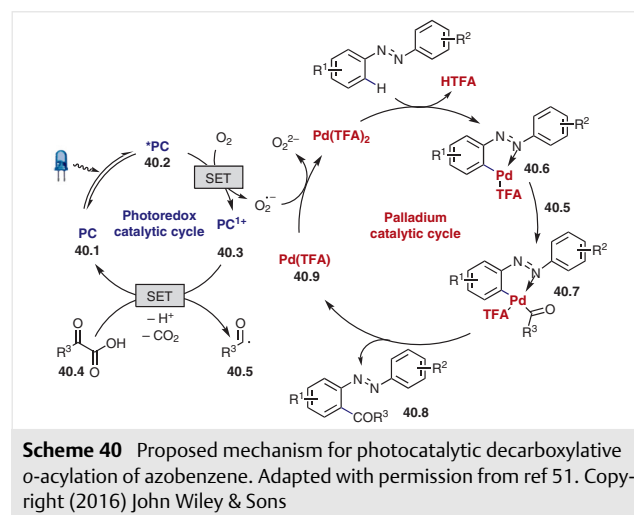
Scheme 38 Proposed mechanism for photocatalytic decarboxylative *o*-acylation⁵⁰

in 77–84% yields. However, no reaction was observed when aliphatic α -oxocarboxylic acid was used as the acyl surrogate. Disubstituted azo- and azoxybenzenes also afforded the desired *o*-acylated products in decent yields (57–78%) regardless of their electronics, however, *o*-disubstituted azo- and azoxybenzene derivatives gave lower yields (37–56%) due to steric problems.



A series of mechanistic studies were conducted to establish the reaction mechanism.⁵¹ A TEMPO trapping experiment suggests the generation of acyl radicals. The intermolecular kinetic isotopic effect observed ($k_H/k_D = 3.7$) in the reaction identifies the C–H activation as the rate-determining step, and an EPR spectroscopic data confirms the generation of a superoxide radical anion ($O_2^{\cdot-}$) in the reaction medium. On the basis of these results, the authors pro-

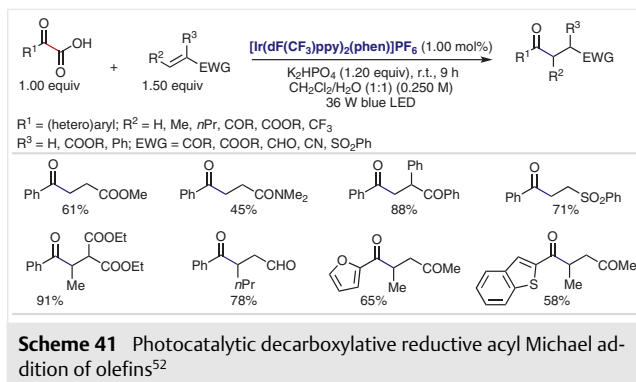
posed a mechanism that begins with the photoexcitation of mesityl acridinium catalyst (PC) **40.1** generating the excited photocatalyst (*PC) **40.2**. Oxidation of **40.2** by molecular oxygen affords PC^{+} **40.3** and a superoxide radical anion. Subsequently, **40.3** oxidizes the α -ketocarboxylic acid to regenerate the ground state photocatalyst PC along with the corresponding carboxyl radical species that leads to the formation of an aroyl radical species **40.5**. On the other side, a Pd catalytic C–H activation of the azobenzene forms the palladacyclic intermediate **40.6**. Addition of the in situ generated radical **40.5** to this palladacyclic intermediate **40.6** affords the Pd^{IV} or Pd^{III} species **40.7** in analogy to the observation of Wang and Li in Scheme 38. At this stage, reductive elimination from **40.7** affords the desired acylated product **40.8** with the formation of the Pd^I intermediate **40.9**, which is further re-oxidized by the superoxide radical anion to regenerate the Pd^{II} catalyst, completing the catalytic cycle (Scheme 40).



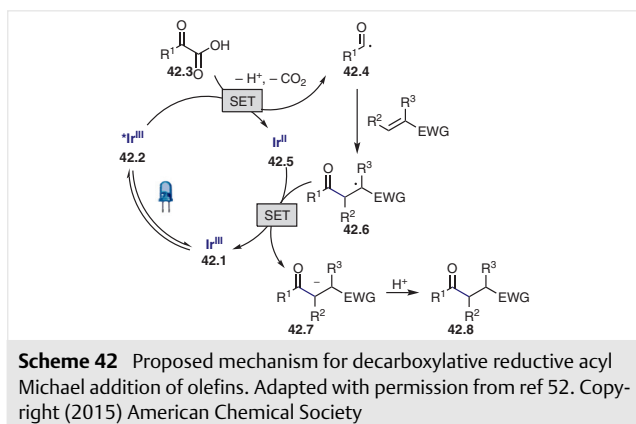
Scheme 40 Proposed mechanism for photocatalytic decarboxylative *o*-acylation of azobenzene. Adapted with permission from ref 51. Copyright (2016) John Wiley & Sons

Acyl radicals, generated by photocatalytic decarboxylation, were also reported by Shang and Fu in 2015 for acyl reductive Michael addition with various Michael acceptors.⁵² Various aromatic and heteroaromatic α -ketocarboxylic acids were decarboxylated in the presence of photoredox catalysts to form (hetero)aroyl radicals. These radicals underwent Michael addition to various α,β -unsaturated esters, ketones, amides, aldehydes, nitriles, and sulfones to afford the corresponding products in 45–94% yields (Scheme 41).

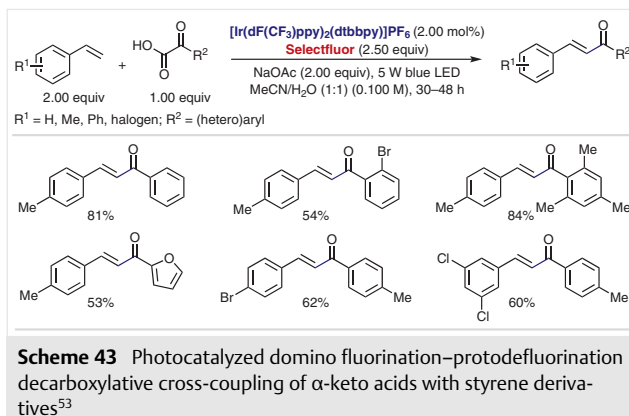
The authors reported that the product yield was significantly decreased by reducing the loading of the base to a catalytic amount, which demonstrates the role of the carboxylate anion in quenching the excited photoredox catalyst.⁵² The reaction has been proposed to proceed via a reductive quenching cycle of photoexcited $^*[\text{Ir}(\text{dF}(\text{CF}_3)\text{ppy})_2(\text{phen})]\text{PF}_6$ (**42.2**) by the α -ketocarboxylate



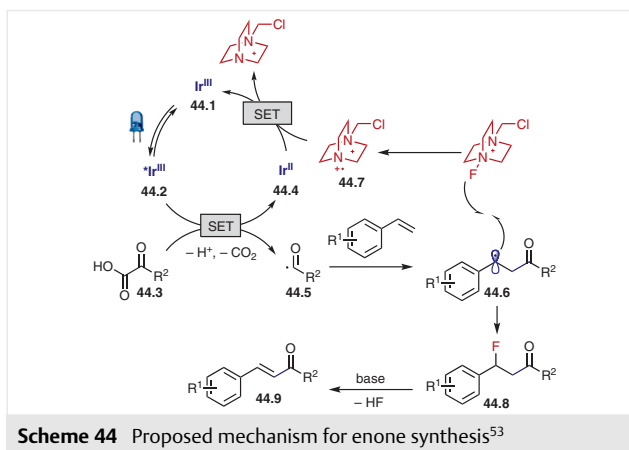
as depicted in Scheme 42. The acyl radical **42.4**, generated via the decarboxylation of an α -ketocarboxylate radical, was subsequently trapped by a Michael acceptor affording the radical **42.6**. This radical oxidizes the Ir^{II} catalyst regenerating the photocatalyst Ir[(dF(CF₃)ppy)₂(phen)]PF₆ and forming the anion **42.7**, which readily protonates to provide the 1,4-addition product **42.8** (Scheme 42). Acrylic acid is an ineffective Michael acceptor under these reaction conditions due to its possible reductive quenching in competition with the 2-ketocarboxylate. β -Dimethylated and β -phenyl-substituted alkene substrates are also incompatible Michael acceptors due to their ability to form stable tertiary or benzylic radicals with a lower oxidation potential to oxidize Ir^{II}.



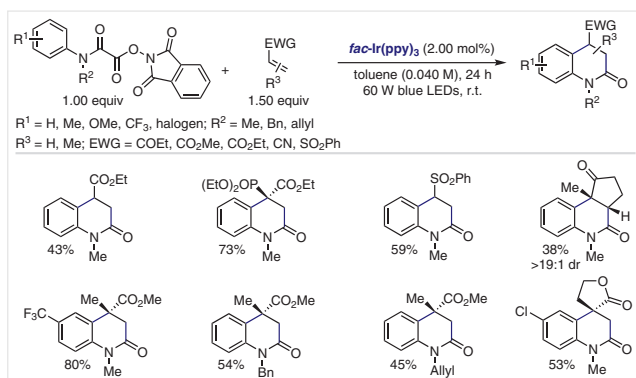
By strategically using the oxidant Selectfluor, Zhu et al. developed a photocatalytic strategy for the synthesis of α,β -unsaturated ketones using α -keto acids and styrene derivatives in 2017.⁵³ With a variety of substituents tolerated on both reactants, this domino fluorination–protodefluorination strategy provides access to the construction of α,β -unsaturated ketones in good yields (50–84%) (Scheme 43). 2-Furanyl-, 2-thienyl-, and 2-naphthyl-substituted α -keto acids all reacted smoothly as the acyl surrogate and gave the corresponding α,β -unsaturated ketones in 50–57% yields.



The use of TEMPO under the standard reaction conditions completely inhibited the product formation, indicating a radical process. The use of the oxidant *t*-butyl hydroperoxide under the standard reaction conditions was unproductive which rules out the possibility of benzylic oxidation. The absence of the base in the optimized reaction conditions provided the desired enone product in 10% yield along with the detection, by NMR analysis, of the fluoro-acylated product. From their observations in control experiments, Zhu⁵³ proposed a mechanism which starts with the visible-light irradiation of the photocatalyst [Ir(dF(CF₃)ppy)₂(dtbbpy)]PF₆ generating a long-lived excited state *Ir^{III} **44.2** (Scheme 44). With the aid of Selectfluor, *Ir^{III} can oxidize the α -keto acid to give the acyl radical species **44.5**, which reacts with styrene derivatives to deliver the benzylic radical **44.6**. Fluorination of **44.6** by Selectfluor produces acyl-fluorinated species **44.8** and the corresponding radical cation **44.7** which oxidizes the reduced Ir^{II} to the ground state Ir^{III} species, thereby completing the photoredox cycle. Finally, the acyl-fluorinated product delivers the final α,β -unsaturated ketone product **44.9** via a base-mediated elimination process.



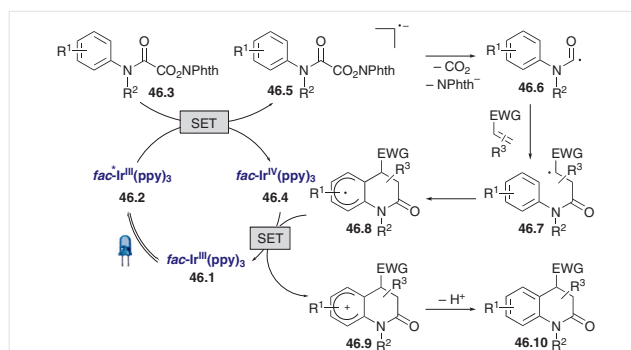
In 2016, Overman's group reported the use of *N*-hydroxyphthalimido esters for the efficient generation of alkyl as well as methoxycarbonyl radicals via a photoredox-catalyzed reductive SET.⁵⁴ Based on this idea, in 2017, Taylor and Donald reported the generation of carbamoyl radicals from *N*-hydroxyphthalimido oxamides and used them for the synthesis of 3,4-dihydroquinolin-2-ones under mild photocatalytic conditions (Scheme 45).⁵⁵ This method provides access to a diverse collection of *o*-, *m*- or *p*-substituted oxamides for the successful generation of 3,4-dihydroquinolin-2-ones in good yields (41–80%). However, a clear trend of increasing yields was observed for oxamides containing electron-withdrawing substituents compared to their electron-donating counterparts. Several mono- and disubstituted alkenes, as well as exocyclic alkenes, all afforded the desired 3,4-dihydroquinolin-2-ones containing fused cyclic (38–81%) and spirocyclic systems (43–71%).



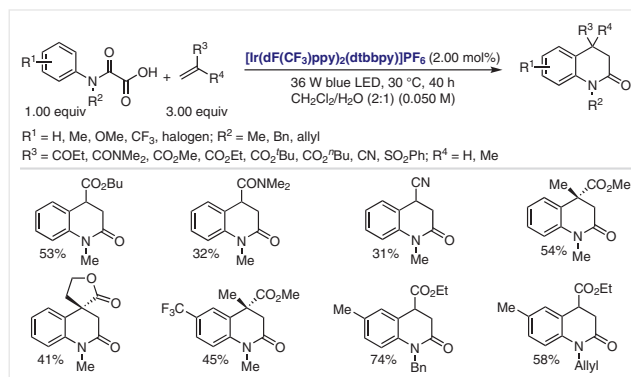
Scheme 45 Photocatalytic intermolecular addition/cyclization for the synthesis of 3,4-dihydroquinolin-2-ones⁵⁵

The proposed mechanistic cycle begins with the irradiation of the photocatalyst fac-Ir(ppy)_3 with visible light, which could lead to the photoexcited state $\text{fac}^*\text{-Ir(ppy)}_3$ (**46.2**). Excited $\text{fac}^*\text{-Ir(ppy)}_3$ ($E_{1/2}^{\text{IV/III}^*} = -1.73 \text{ V vs SCE}$)⁵⁶ reduces the *N*-hydroxyphthalimido oxamide **46.3** to form the radical anion **46.5**, which rapidly fragments releasing CO₂, NPhth⁻, and the carbamoyl radical **46.6**. The carbamoyl radical undergoes Michael addition to an electron-deficient olefin followed by cyclization to produce cyclohexadienyl radical **46.8**. Oxidation of **46.8** by the photocatalyst ($E_{1/2}^{\text{IV/III}} = +0.77 \text{ V vs SCE}$)⁵⁶ forms cyclohexadienyl cation **46.9**, which is deprotonated and rearomatized to give 3,4-dihydroquinolin-2-one **46.10** along with simultaneous regeneration of the ground state Ir^{III} catalyst (Scheme 46).

In contrast to the earlier reductive approach to the generation of a carbamoyl radical from an oxamide (Scheme 45), Feng et al. reported, in 2018, a photocatalytic oxidative decarboxylation approach by taking oxamic acids as the carbamoyl precursor for the synthesis of analogous 3,4-di-



Scheme 46 Proposed mechanism for the photocatalytic synthesis of 3,4-dihydroquinolin-2-ones. Adapted with permission from ref 55. Copyright (2017) American Chemical Society

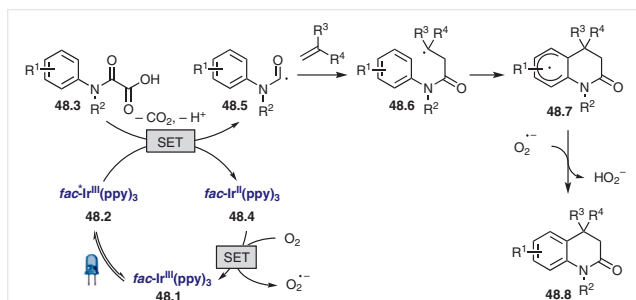


Scheme 47 Photocatalytic synthesis of 3,4-dihydroquinolin-2(1H)-ones using oxamic acids⁵⁷

hydroquinolin-2(1H)-ones (Scheme 47).⁵⁷ A variety of electron-donating and electron-withdrawing oxamic acids are compatible with the reaction under the optimized conditions, affording a wide variety of 3,4-dihydroquinolin-2(1H)-ones in moderate (41–74%) yields. A range of mono, disubstituted and exocyclic alkenes are compatible with these reaction conditions leading to the desired products containing fused cyclic (31–60%) and spirocyclic systems (41%).

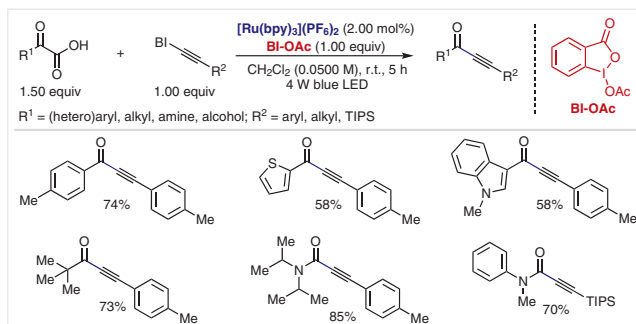
From the reaction of *N*-methyl-*N*-phenyloxamic acid with ethyl acrylate under the standard conditions, a trace amount of *N*-methyl-*N*-phenylformamide was isolated, and the addition of the radical scavenger TEMPO to the standard reaction mixtures gave only a trace amount of the desired product. Both of these results indicate the formation of a carbamoyl radical in the reaction medium. On the basis of these results, the authors proposed a mechanistic cycle in which the photoexcited catalyst Ir^{III} **48.2** undergoes a reductive quenching to generate Ir^{II} and carbamoyl radical intermediate **48.5** (Scheme 48). Analogous to Scheme 46, addition of the carbamoyl radical to the electron-deficient olefin followed by intramolecular cyclization forms a cyclohexadienyl radical intermediate **48.7**. Final oxidation of reduced Ir^{II} by molecular oxygen affords the ground state Ir^{III}

and a superoxide radical anion, which abstracts a hydrogen atom from cyclohexadienyl radical **48.7** to deliver the desired 3,4-dihydroquinolin-2(1*H*)-one **48.8**.



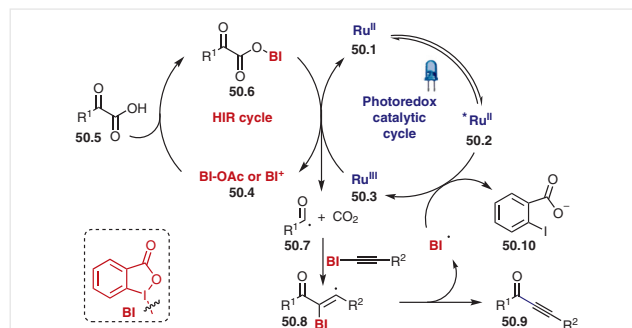
Scheme 48 Proposed mechanism for the synthesis of 3,4-dihydroquinolin-2(1*H*)-ones⁵⁷

The combination of visible-light photocatalysis with hypervalent iodine reagents (HIR) was successfully employed by Chen et al. in 2015 for the generation of an acyl radical.⁵⁸ This chemoselective decarboxylative alkylation strategy shows a broad substrate scope in terms of HIR-bound alkynes as well as the α -keto acids. Aryl-substituted benziodoxolonyl-alkynes (BI-alkynes) containing electron-donating and electron-withdrawing substituents as well as alkyl-bound BI-alkynes all reacted well to deliver the desired alkynylated products in 65–93% and 65–85% yields, respectively (Scheme 49). The triisopropylsilyl (TIPS)-substituted BI-alkynes, which can be easily deprotected to generate terminal alkynones, also provided good (61–70%) yields of the desired products. Irrespective of steric and electronic effects, substituted alkyl, aryl, and heteroaryl α -keto acids were well tolerated and afforded the desired products in 57–87% yields. Aryl α -keto acid substrates bearing sensitive functional groups such as allyl esters, propargyl esters, alcohols, and azides were also well tolerated under these reaction conditions giving the desired alkynylated products in 62–74% yields.



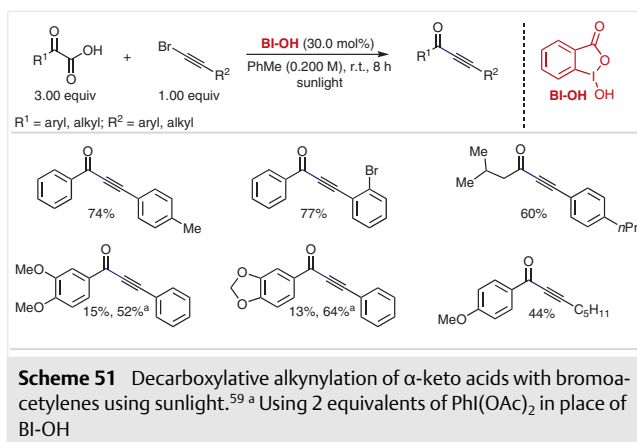
Scheme 49 Photocatalytic decarboxylative alkylation using α -keto acids⁵⁸

NMR studies and the formation of alkynylation products using a BI-keto acid complex in place of α -keto acids and BI-OAc, under otherwise identical reaction conditions, confirms the formation of a BI-keto acid complex in the reaction medium. The luminescence quenching of $[\text{Ru}(\text{bpy})_3]^{2+}$ was much weaker in the presence of the α -keto acid compared to BI-OAc, indicating that BI-OAc is primarily the oxidative quencher in this reaction. In accordance with observations from control experiments, the authors proposed that the benziodoxole-oxoacid complex **50.6** (BI-O₂CCOR¹), generated in situ from an α -keto acid and BI-OAc, is oxidized by Ru^{III} to liberate carbon dioxide, a benziodoxole cation (BI⁺ or BI-OAc), $[\text{Ru}(\text{bpy})_3]^{2+}$ and the aroyl radical **50.7** (Scheme 50).⁵⁸ The aroyl radical undergoes α -addition to the BI-alkyne followed by elimination of a benziodoxolonyl radical (BI[•]) to yield the alkynone **50.9**. BI[•] oxidizes the photoexcited $^*[\text{Ru}(\text{bpy})_3]^{2+}$ to complete the photoredox cycle.

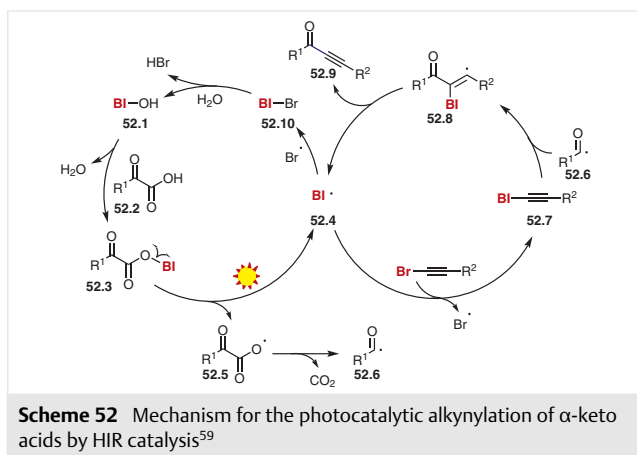


Scheme 50 Mechanism for alkynylation using HIR and photoredox catalysis. Adapted with permission from ref 58. Copyright (2015) John Wiley & Sons

In 2015, Li and Wang used a BI-OH reagent instead of BI-OAc to activate α -ketocarboxylic acids for the successful development of sunlight-driven decarboxylative alkylation.⁵⁹ A range of aromatic α -keto acids reacted with (bromoethynyl)benzene under the optimized conditions to afford the corresponding alkynones in 44–76% yields. 4-Methyl-2-oxopentanoic acid, an aliphatic α -keto acid, reacted with a series of *o*-, *m*- and *p*-substituted 2-aryl-1-bromoethynes to provide the desired products in good yields (60–74%). Irrespective of steric and electronic effects, substituted bromoacetylenes, when reacting with 2-keto-2-phenylacetic acid, form the desired products in 65–80% yields (Scheme 51). The presence of two strongly electron-donating groups (–OR) on the aromatic ring of the 2-keto-2-arylacetic acid, such as in 2-(3,4-dimethoxyphenyl)-2-ketoacetic acid and 2-(benzo[*d*][1,3]-dioxol-5-yl)-2-oxoacetic acid, when reacted with (bromoethynyl)benzene afforded the desired products in only 15% and 13% yields, respectively. However, replacing the catalytic BI-OH with a stoichiometric amount of PhI(OAc)₂ improved the yields of these two products to 52% and 64%, respectively.

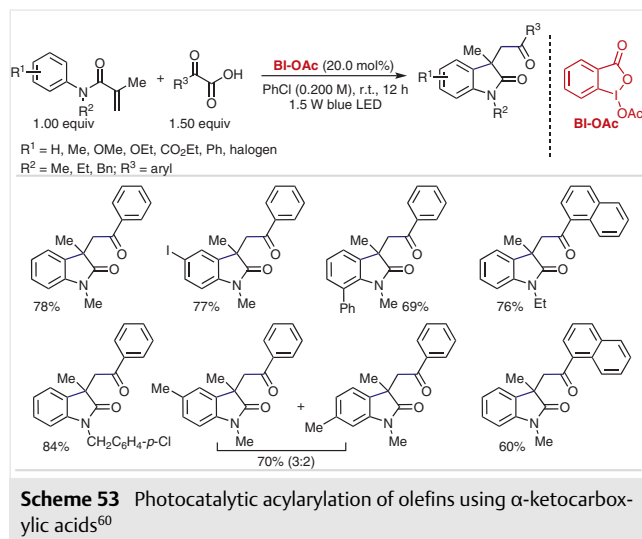


The trapping of a TEMPO adduct in the presence of TEMPO and trapping of the benzoyl as well as the benziodoxolonyl radicals by BHT under the standard conditions confirms the formation of benziodoxolonyl and benzoyl radicals in the reaction medium. Using an equivalent amount of BI-alkyne and α -keto acid, the desired product was obtained in 66% yield only in the presence of 30% of the BI-OH (HIR) catalyst. Separately synthesized BI-keto acid (BI-OCOCOPh), when reacted with bromoacetylenes, gave a good yield of the desired product. These results indicate the involvement of BI-alkynes and a BI-keto acid complex in this reaction. From these mechanistic studies, it was proposed that BI-OH (**52.1**) reacts with the ketocarboxylic acid **52.2** to form the BI-oxoacid complex **52.3** (Scheme 52). This complex generates the benziodoxolonyl radical (**52.4**) and a ketocarboxyl radical **52.5** under irradiation by sunlight. Subsequently, **52.4** reacts with bromoalkyne to give the BI-alkyne **52.7** and releases a Br radical. At the same time, decarboxylation of **52.5** produces an aroyl radical that adds to the BI-alkyne to form **52.8**, which releases the alkynone product **52.9** and the benziodoxolonyl radical. This radical

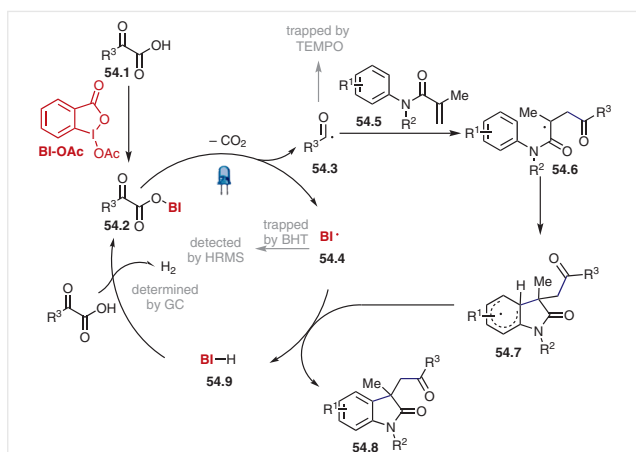


recombines with the Br radical, and this is followed by hydrolysis to regenerate BI-OH and complete the catalytic cycle.

In 2016, Wang et al. reported BI-OAc as an efficient HIR catalyst for the decarboxylative 1,2-acylarylation/tandem cyclization of acrylamides with α -ketocarboxylic acids in the presence of only visible light (Scheme 53).⁶⁰ Regardless of steric and electronic effects, various *N*-methyl-*N*-arylmethacrylamides as well as aromatic ketocarboxylic acids afforded the desired products in moderate to good (58–78%) yields. Methyl substitution at the *m*-position of the *N*-methyl-*N*-arylmethacrylamide provided a regioisomeric product (70%) in a 3:2 ratio, but acrylamides containing a free amine or alcohol failed to couple under the reaction conditions. Rather than *N*-methyl-*N*-arylmethacrylamides, other acrylamides such as *N*-ethyl-*N*-arylmethacrylamide and *N*-benzyl-*N*-arylmethacrylamide formed the desired products in 70–84% yields. However, *N*-phenyl-*N*-arylmethacrylamide was unproductive under the optimized reaction conditions.



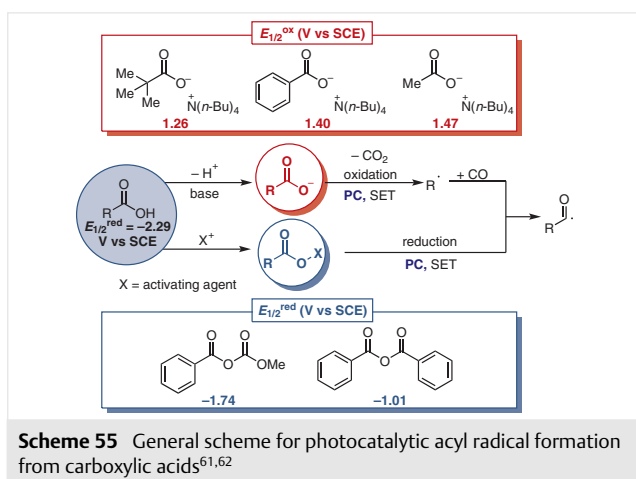
The catalytic cycle is initiated by the reaction of BI-OAc and the ketocarboxylic acid **54.1** to generate the BI-keto acid intermediate **54.2**. Visible-light-mediated homolytic cleavage of the BI–O bond of **54.2** liberates CO_2 , a benzoyl radical **54.3**, and a benziodoxolonyl radical (**54.4**). Addition of **54.3** across the double bond of arylmethacrylamides **54.5** followed by cyclization gives intermediate **54.7**, which undergoes hydrogen atom abstraction by **54.4** to deliver the desired 3,3-disubstituted 2-oxindole **54.8** and BI-H (**54.9**). The reaction of **54.9** with the ketocarboxylic acid **54.1** liberates hydrogen gas and generates the BI-oxo acid intermediate **54.2** for the next cycle (Scheme 54).



Scheme 54 Proposed mechanism for photocatalytic acylarylation of olefins⁶⁰

5 Carboxylic Acids as a Source of Acyl Radicals

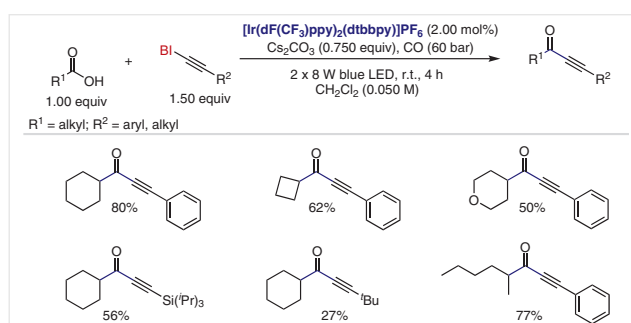
Simple and inexpensive carboxylic acids can be an alternative source from which to generate the acyl radical by visible-light photoredox catalysis (PC). Base-mediated photocatalytic oxidation, decarboxylation and further carbonylation of the in situ generated alkyl radical by carbon monoxide (CO) can afford acyl radicals. Alternatively, the carboxylic acid is converted into its redox-active ester by the use of an activating agent (X = active electrophile) which can be reduced by the photoredox catalyst (PC) to form the acyl radical (Scheme 55). The redox properties of some carboxylates and anhydrides are listed in Scheme 55.^{61,62}



Scheme 55 General scheme for photocatalytic acyl radical formation from carboxylic acids^{61,62}

In 2015, Lu and Xiao reported a visible-light photocatalytic decarboxylative–carbonylative alkylation of carboxylic acids with hypervalent iodine bound alkynes in the presence of carbon monoxide.⁶³ A range of cyclic and acyclic aliphatic carboxylic acids exhibited good reactivity in this

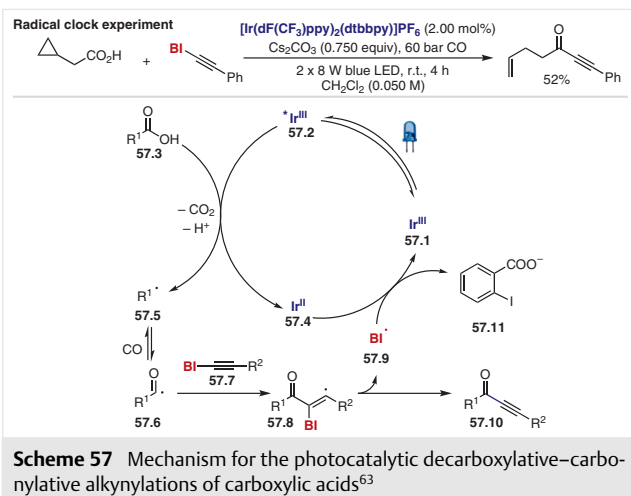
radical carbonylative alkylation giving the desired products in 42–90% yield. Rather than aromatic BI-alkynes (BI = benzyldoxolonyl), tri-isopropylsilyl- and *t*-butyl-substituted BI-alkynes also provided the desired products in moderate (27–56%) yields when reacted with cyclohexyl carboxylic acid (Scheme 56). Benzoic acids failed to react, which is likely due to the slower decarboxylation of the benzoates to aryl radicals under the reaction conditions⁶⁴ (rate constants for the decarboxylation (s^{-1}): aryl carboxylic radical:⁶⁵ $1.4 \pm 0.3 \times 10^6$; alkyl carboxylic radical:⁶⁴ 2.2×10^9). α -Amino- and α -oxygen-substituted carboxylic acids were also incompatible with the reported reaction conditions.



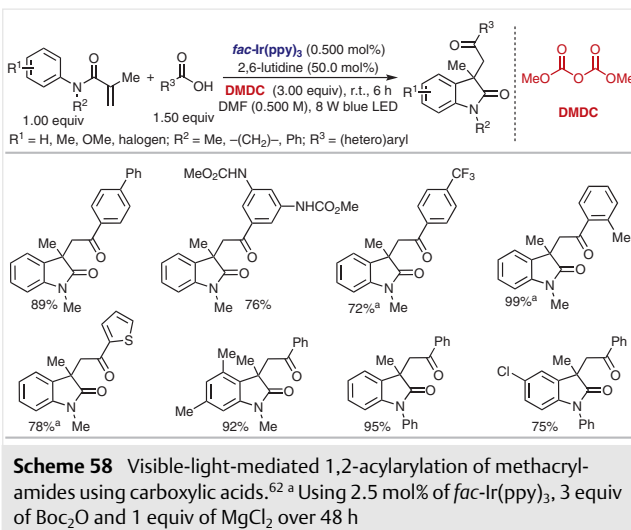
Scheme 56 Visible-light-induced decarboxylative–carbonylative alkylations of carboxylic acids⁶³

The use of 2-cyclopropylacetic acid as the carboxylic acid substrate afforded a ring-opened alkene-alkyne product in 52% yield under the standard reaction conditions, which confirms the intermediacy of an alkyl radical. On the basis of this radical clock experiment, the author proposed a tentative mechanism, in which the excited state $^*Ir^{III}$ photocatalyst ($E_{1/2}^{III^{III}} = +1.21$ V vs SCE)⁴⁶ **57.2** reacts with carboxylic acid **57.3** [$E_{1/2}^{red}$ (cyclohexyl carboxylate) = +1.18 V vs SCE]⁶³ to form the alkyl radical **57.5** with the release of CO_2 . This alkyl radical further produces acyl radical **57.6** in the presence of carbon monoxide. Addition of this acyl radical to the BI-alkyne **57.7** followed by the release of the BI radical (**57.9**) provides the alkynone product **57.10**. The BI radical oxidizes Ir^{II} to regenerate the ground state Ir^{III} photocatalyst and form the carboxylate **57.11** (Scheme 57).

In 2015, Wallentin et al. employed for the first time the activating agent dimethyl dicarbonate (DMDC) to generate an acyl radical from carboxylic acids using visible-light photocatalysis (Scheme 58).⁶² A range of substituted methacrylamides, when reacted with benzoic acid under the standard reaction conditions, afforded the 3,3-disubstituted 2-oxindole derivatives in good to excellent yields (74–95%). Benzoic acids bearing substituents at the *o*-, *m*- or *p*-position as well as carboxylic acids with extended aromatic systems all reacted very well (76–97%) under the optimized reaction conditions. Surprisingly, *o*- and *p*-methyl-, as well as *p*-hydroxy- and *p*-trifluoromethylbenzoic acids reacted

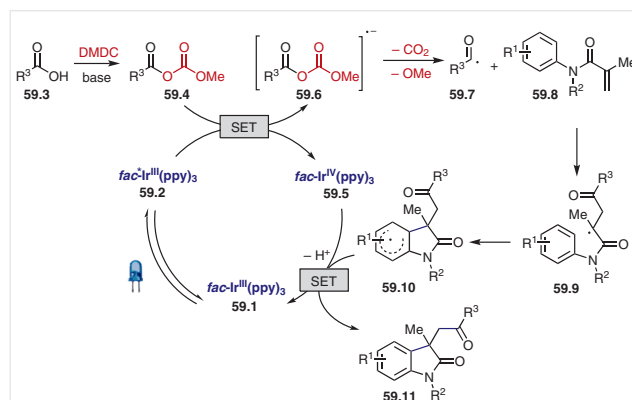


very poorly under the standard conditions, however, after replacing DMDC with Boc_2O and 1 equivalent of MgCl_2 and increasing the loading of $\text{fac-Ir}(\text{ppy})_3$ to 2.5 mol%, the desired products were produced in good (72–99%) yields. These new reaction conditions [Boc_2O , 1 equiv of MgCl_2 and 2.5 mol% of $\text{fac-Ir}(\text{ppy})_3$] were very effective for heteroaromatic carboxylic acids and afforded the 1,2-acylarylation products in good (33–78%) yields.

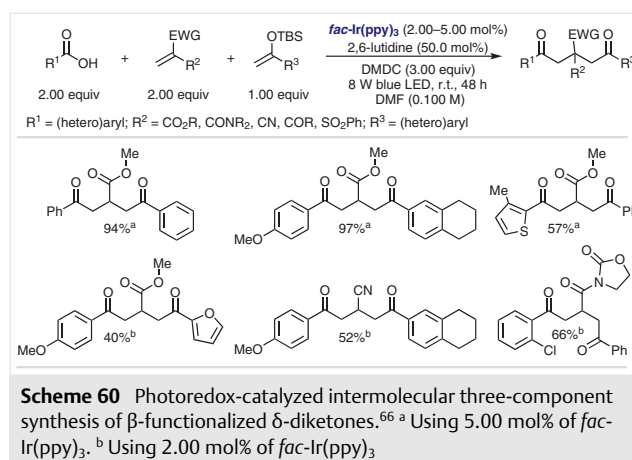


When a mixed anhydride synthesized separately from the reaction of benzoic acid and DMDC reacted with methacrylamides under the standard reaction conditions, the desired product was formed in a good yield. Stern–Volmer fluorescence quenching studies clearly revealed that anhydrides quench the excited $\text{fac-Ir}(\text{ppy})_3$. From these mechanistic studies, a plausible mechanism was derived and is depicted in Scheme 59. The photoexcited $\text{fac-Ir}(\text{ppy})_3$ **59.2** ($E_{1/2}^{\text{IV/III}} = -1.73 \text{ V vs SCE}$) reduces the anhydride **59.4**, gen-

erated in situ from the carboxylic acid **59.3** in the presence of DMDC and 2,6-lutidine, to produce $\text{fac-Ir}^{\text{IV}}(\text{ppy})_3$ (**59.5**) and a radical anion **59.6**. Decarboxylation of **59.6** gives the acyl radical **59.7**, which adds to the double bond of the methacrylamide **59.8** and subsequently undergoes cyclization to afford intermediate **59.10**. Oxidation of **59.10** by $\text{fac-Ir}^{\text{IV}}(\text{ppy})_3$ provides the desired product **59.11** with regeneration of the photocatalyst $\text{fac-Ir}(\text{ppy})_3$ to close the catalytic cycle.

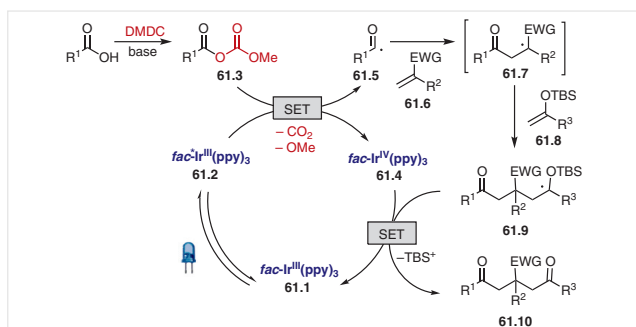


In 2017, the Wallentin group merged the concept of photocatalytic acyl radical formation from carboxylic acids with multicomponent reactions (Scheme 60).⁶⁶ Strategically combining electron-poor and electron-rich alkenes with acyl radicals generated from mixed anhydrides of DMDC and carboxylic acids, the method was able to provide access to the synthetically challenging 1,2-dicarbonylation of alkenes. This strategy yielded 1,2-difunctionalized products in good (33–97%) yields when reacted with substituted aromatic as well as heteroaromatic carboxylic acids with different silanol ethers and methyl acrylate. The scope of the reaction was further extended to other electron-poor



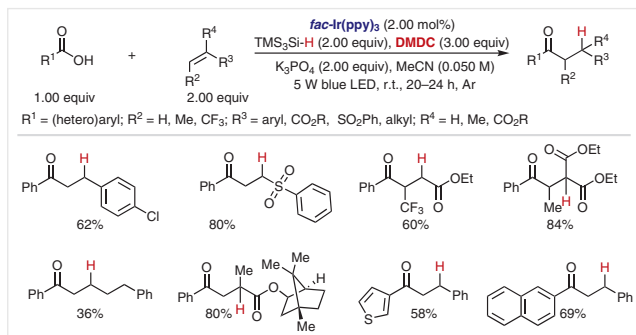
olefins beyond methyl acrylates, with these reactions affording the desired difunctionalized products in 41–66% yields.

The reaction pathway for the formation of the acyl radical **61.5** is the same as that proposed in Scheme 59. The nucleophilic acyl radical first adds to the electron-poor olefin **61.6** forming the radical intermediate **61.7** (Scheme 61). This electron-deficient radical species reacts selectively with silyl enol ether **61.8** to deliver **61.9**, which is oxidized by $fac\text{-Ir}^{\text{IV}}(\text{ppy})_3$ and this is followed by desilylation to produce the desired product **61.10**.



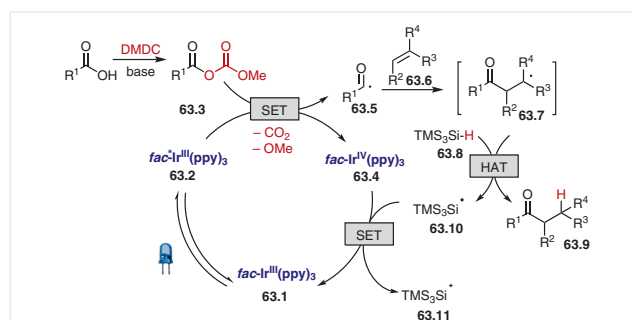
Scheme 61 Proposed mechanism for the photoredox-catalyzed intermolecular three-component synthesis of β -functionalized δ -diketones⁶⁶

Using the idea of in situ generation of anhydrides as the acyl radical precursors, Zhu's group reported three photocatalytic reactions in 2017.^{67–69} First, they reported the photoredox-catalyzed hydroacylation reaction of olefins using carboxylic acids as acyl radical precursors and tris(trimethylsilyl)silane ($\text{TMS}_3\text{Si-H}$) as a hydrogen atom source (Scheme 62).⁶⁷ A range of electron-donating and electron-withdrawing substituted styrenes, such as α,β -substituted or unsubstituted vinyl esters, a vinyl sulfone, and an aliphatic olefin all reacted well with benzoic acid to afford the corresponding hydroacylated products in 36–84% yields. Both aromatic and heteroaromatic carboxylic acids were viable substrates and coupled with styrene to give the desired products in 53–70% yields.



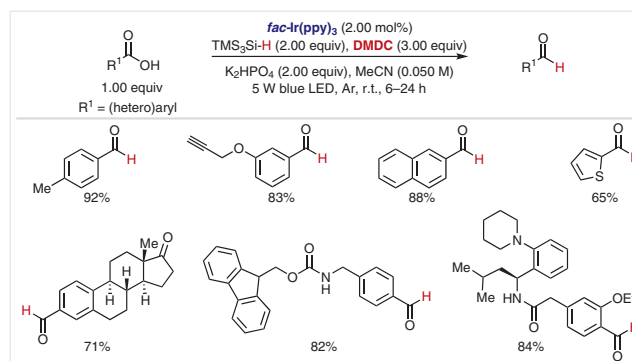
Scheme 62 Photocatalytic hydroacylation of olefins using carboxylic acids and hydrosilanes⁶⁷

TEMPO additives completely shut down this hydroacylation reaction, which indicates the radical nature of this process (Scheme 63). The mechanism starts with the excitation of $fac\text{-Ir}(\text{ppy})_3$ **63.1** to excited $fac\text{-}^*\text{Ir}(\text{ppy})_3$ **63.2** by visible-light irradiation. Single-electron reduction of the mixed anhydride **63.3**, generated by reacting the carboxylic acid with DMDC, by the excited $fac\text{-}^*\text{Ir}(\text{ppy})_3$ forms acyl radical **63.5** with the extrusion of CO_2 and OMe . Subsequent addition of the acyl radical to the activated olefins forms radical intermediate **63.7**. This radical intermediate then quickly abstracts the proton from $\text{TMS}_3\text{Si-H}$ **63.8** to give the desired hydroacylation product **63.9**. The final SET process between $fac\text{-Ir}^{\text{IV}}(\text{ppy})_3$ and **63.10** regenerates the ground state $fac\text{-Ir}(\text{ppy})_3$ for the next cycle.

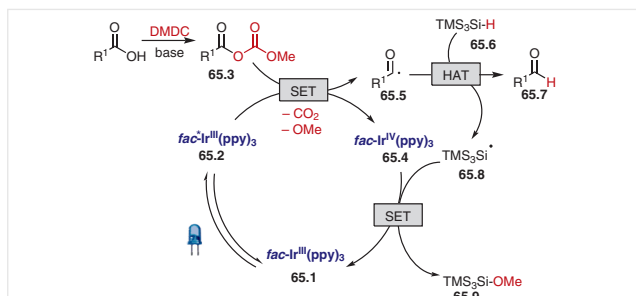


Scheme 63 Proposed mechanism for the photocatalytic hydroacylation of olefin.⁶⁷ Adapted with permission from ref 67. Copyright (2017) American Chemical Society

Shortly after their photocatalytic hydroacylation of activated alkenes, Zhu et al. reported the selective photocatalytic reduction of aromatic carboxylic acids to the corresponding aldehydes using the $fac\text{-Ir}(\text{ppy})_3$ and tris(trimethylsilyl)silane ($\text{TMS}_3\text{Si-H}$) system (Scheme 64).⁶⁸ Aromatic carboxylic acids, regardless of the position and electronic properties of the substituents including free alkynyl, amide, and ester groups, reacted smoothly under the optimized reaction conditions to afford the corresponding aldehydes in 82–92% yields. Heteroaromatic carboxylic acids and a few complex aryl carboxylic acids were successfully reduced to



Scheme 64 Photocatalytic reduction of carboxylic acids to aldehydes⁶⁸

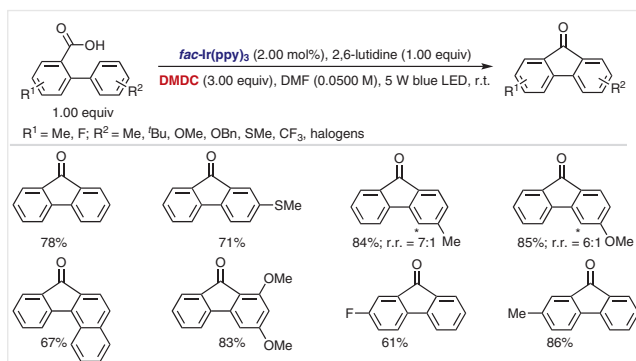


Scheme 65 Proposed mechanism for the photocatalytic reduction of carboxylic acids⁶⁸

the desired aldehydes as well. However, aliphatic carboxylic acids such as 3-phenylpropanoic acid, cyclohexane carboxylic acid, and *N*-Boc-glycine were all unproductive under the standard reaction conditions.

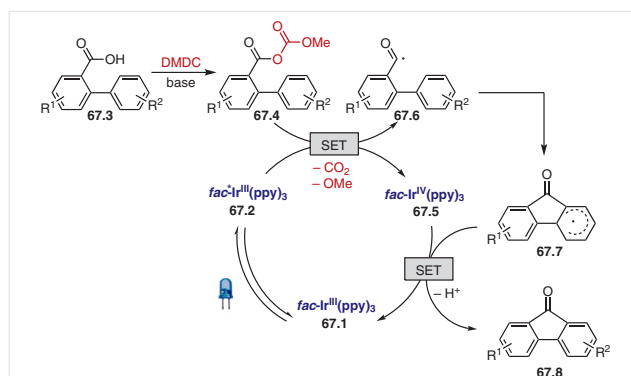
The proposed mechanism up to the formation of the acyl radical **65.5** by excited $fac\text{-}^*Ir(ppy)_3$ **65.2** (Scheme 65) is the same as the hydroacylation reaction mechanism using carboxylic acids (Scheme 63). Once the reactive acyl radical **65.5** is generated, it rapidly reacts with TMS_3Si-H (**65.6**) to form the corresponding aldehyde **65.7**. Regeneration of $fac\text{-}Ir(ppy)_3$ occurs in the final stage by the reaction of $fac\text{-}Ir^{IV}(ppy)_3$ and **65.8**.

The third reaction developed by Zhu's group in 2017 was an efficient deoxygenative intramolecular acylation/radical cyclization via photoredox catalysis for the synthesis of valuable fluorenone products.⁶⁹ A variety of functionalized biarylcarboxylic acids containing *o*- and *p*-substituents on the 2-aryl ring afforded fluorenones in 54–85% yields, while the *m*-substituted aromatics gave regioisomeric products. Electron-donating or electron-withdrawing substituents on the aromatic moiety of the carboxylic acid were well tolerated under the standard reaction conditions (61–86%) (Scheme 66).



Scheme 66 Photocatalytic intramolecular acylation/radical cyclization of biarylcarboxylic acids;⁶⁹ r.r. = regioisomeric ratio

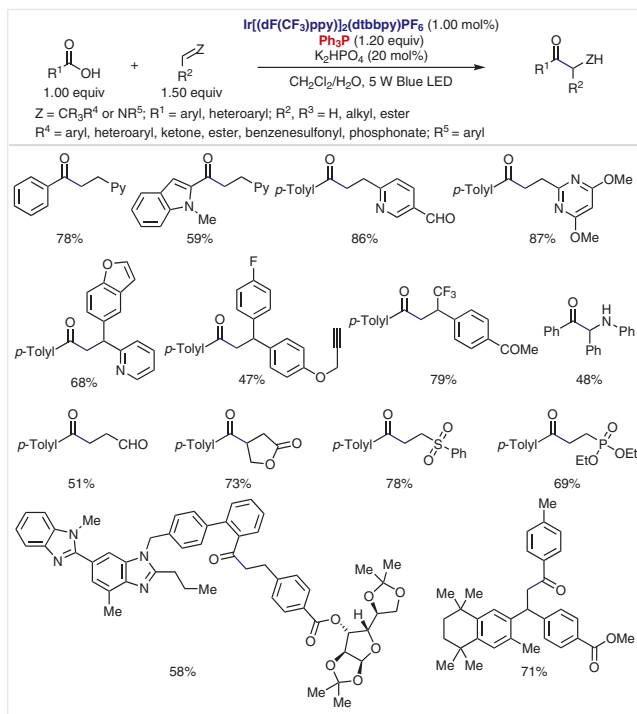
A plausible mechanism for this intramolecular radical cyclization process is shown in Scheme 67. The acyl radical **67.6** generated from the mixed anhydride **67.4** adds to the *ortho* position of the 2-aryl ring to give intermediate **67.7**. Oxidation of intermediate **67.7** by $fac\text{-}Ir^{IV}(ppy)_3$ followed by deprotonation regenerates the ground state $Ir(ppy)_3$ and affords the desired product **67.8**.



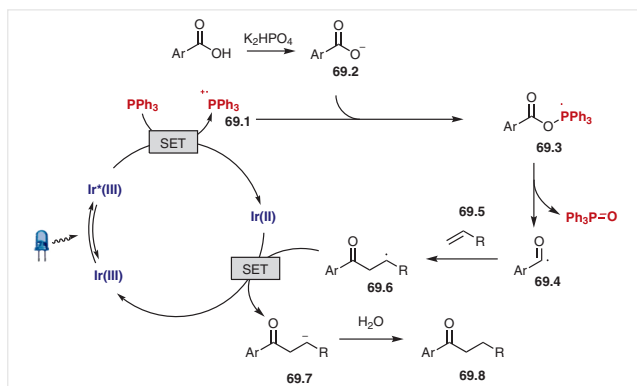
Scheme 67 Mechanism for the intramolecular acylation/radical cyclization⁶⁹

In 2018, Zhu et al. merged phosphoranyl radical chemistry with photoredox catalysis to form acyl radicals from carboxylic acids via C–O cleavage using Ph_3P or Ph_2POEt . These acyl radicals added to alkenes and imines to give the desired hydroacylation products (Scheme 68).⁷⁰ The scope of the reaction is very broad. Various aryl and heteroaryl carboxylic acids reacted with a wide array of electronically diverse alkenylpyridines, styrenes, and Michael acceptors such as acrylate, phenyl vinyl sulfone, diethyl vinylphosphonate, cyclohexanone and lactones to give the desired ketones in 38–89% yields. However, alkyl, alkenyl, and alkynyl carboxylic acids failed to give the desired products. Notably, the reaction is amenable to late-stage functionalization of complex carboxylic acids and alkenes in yields of 40–76%. The reaction is also applicable to the hydroacylation of imines generated in situ under the reaction conditions to afford α -amino-ketone products.

Based on a series of mechanistic studies including radical trapping, deuterium- and ^{18}O -labeling, and Stern–Volmer quenching experiments, a proposed reaction mechanism is depicted (Scheme 69). Photoexcited $Ir^*[(dF(CF_3)ppy)_2(dtbbpy)PF_6]$ ($E_{1/2}^{III/II} = +1.21$ V vs SCE)⁴⁶ undergoes reductive quenching by PPh_3 ($E_{1/2}^{red} = +0.98$ V vs SCE)⁷¹ to form Ir^{II} and the triphenylphosphine radical cation **69.1**. Deprotonation of an aryl or heteroaryl carboxylic acid by K_2HPO_4 forms a carboxylate, which reacts with **69.1** to form a phosphoranyl radical **69.3**. β -Scission of the phosphoranyl radical **69.3** liberates triphenylphosphine oxide and acyl radical **69.4**, which then adds to olefin **69.5** to deliver the alkyl radical intermediate **69.6**. Reduction of **69.6** by Ir^{II}



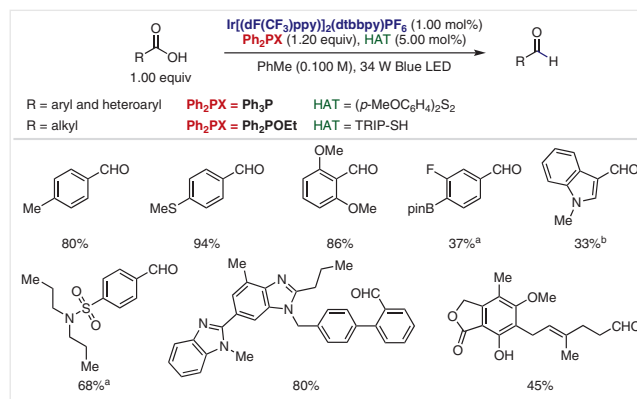
Scheme 68 Substrate scope of the hydroacylation of alkenes and imines under photocatalytic conditions using Ph_3P as a deoxygenating reagent⁷⁰



($E_{1/2}^{\text{III}/\text{II}} = -1.37 \text{ V vs SCE}$)^{15a} regenerates the Ir^{III} photoredox catalyst and anion **69.7**, which undergoes protonation to give the desired ketone **69.8**.

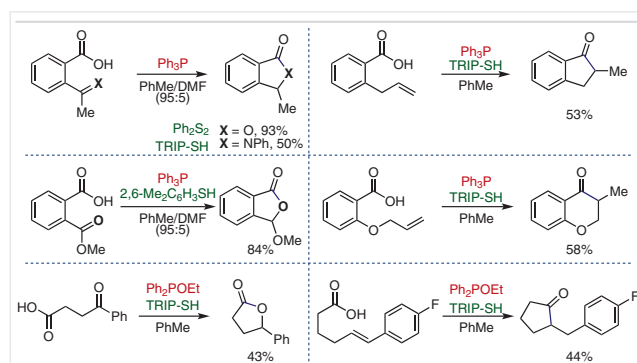
Concurrently and independently, Doyle et al. (Scheme 70) applied the same concept for converting alkyl, aryl, and heteroaryl carboxylic acids into the corresponding acyl radicals,⁷² which abstract a hydrogen atom from arylthiols to form the desired aldehydes. The scope of the reaction is quite general: electron-rich and electron-deficient aryl car-

boxylic acids, heteroaryl carboxylic acids with indole, benzothiofene and quinolone, and aliphatic carboxylic acids all reacted under the optimized conditions to form the corresponding aldehydes in 34–94% yields.



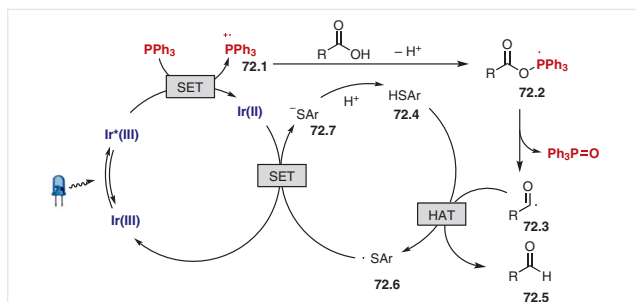
Scheme 70 Substrate scope of the photocatalytic deoxygenative approach for aldehyde formation from carboxylic acids.^{72 a} 2,6-Lutidine was added (1.00 equiv), ^b *N*-methyl-2-pyrrolidone (NMP) was used as the solvent

When radical acceptors such as carbonyl and iminyl derivatives or alkenes were *ortho* to the carboxylic acid group on a benzene ring, intramolecular acyl radical addition took place to form cyclized products in 50–93% yields (Scheme 71). Aliphatic carboxylic acids could cyclize to form five-membered lactone and ketone products in 43% and 44% yields, respectively.



Scheme 71 Intramolecular cyclization of acyl radicals and radical acceptors under photocatalytic conditions⁷²

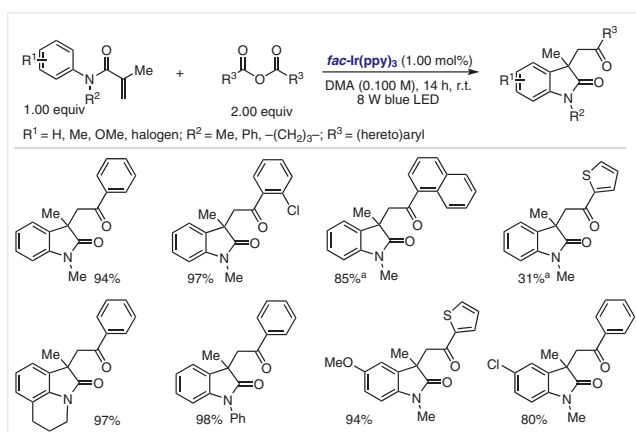
Generation of the acyl radical is similar to the mechanism proposed by Zhu (Scheme 69).⁷⁰ Once the acyl radical **72.3** is formed, it abstracts a hydrogen atom from an arylthiol **72.4** to give the desired aldehyde **72.5** and an arylthiyl radical **72.6** (Scheme 72). Reduction of **72.6** by Ir^{II} regenerates the Ir^{III} photoredox catalyst and thiolate **72.7**, which upon protonation forms the arylthiol **72.4**.



Scheme 72 Proposed mechanism for the photocatalytic acyl radical formation using Ph_3P as a deoxygenating reagent.⁷²

6 Anhydrides as a Source of Acyl Radicals

Rather than the in situ formation of anhydrides from carboxylic acids in the presence of DMDC or Boc_2O , the direct use of anhydrides is an alternate means of generating acyl radicals using visible-light photoredox catalysis. In 2016, Wallentin et al. employed aromatic carboxylic anhydrides as the direct acyl radical source for olefinic radical acylation under photocatalytic conditions.⁷³ The method efficiently yielded 3,3-disubstituted 2-oxindoles (45–98%) using a variety of symmetrical electron-withdrawing aromatic anhydrides. This protocol was also applied to variously substituted *N*-phenylacrylamides to give the corresponding products in 80–98% yields (Scheme 73). Interestingly, the Lewis acid activation of more challenging electron-rich aromatic and heteroaromatic carboxylic anhydrides was found to be necessary for the generation of the corresponding carbonyl radicals and the efficient synthesis of the desired products in 31–95% yields.

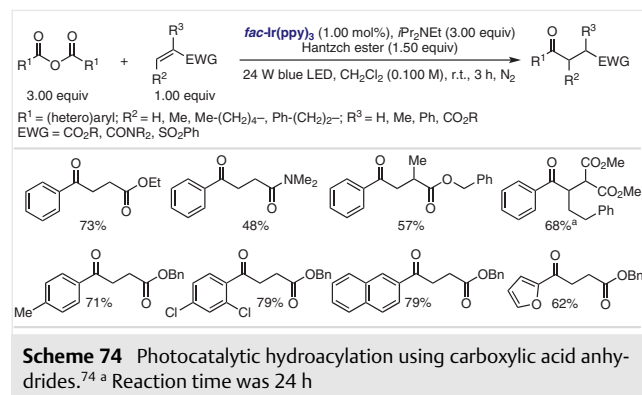


Scheme 73 Photocatalytic 1,2-acylation of olefins using anhydrides.⁷³ ^a Reaction performed by adding 1 equivalent of MgCl_2 ; reaction time = 60 h

Stern–Volmer experiments indicate that the emission intensity of excited $\text{fac-}^*\text{Ir}(\text{ppy})_3$ [$E_{1/2}^{\text{IV/III}} = -1.73$ V vs SCE] was quenched significantly in the presence of symmetrical

anhydrides (benzoic anhydride: $E_{1/2}^{\text{red}} = -1.01$ V vs SCE).⁶¹ The plausible mechanism is analogous to Wallentin's previous mechanism for 1,2-acylation of methacrylamide (Scheme 59),⁶² except the anhydride is directly employed here rather than being generated in situ from a carboxylic acid.

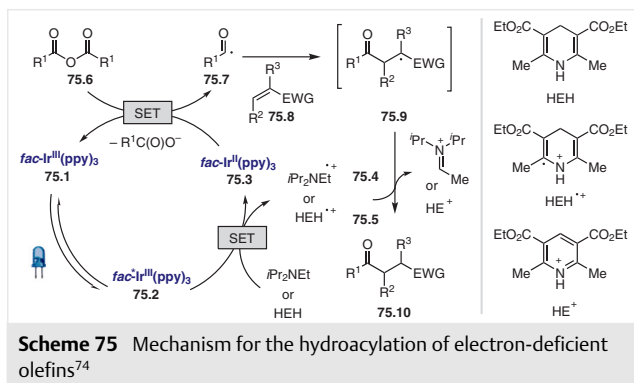
Following the Wallentin group's report on the direct use of anhydrides as the acyl radical surrogate under photoredox conditions, Ye et al., in 2017, reported the construction of 1,4-dicarbonyl compounds using analogous symmetrical carboxylic anhydrides or mixed anhydrides.⁷⁴ A wide range of symmetrical anhydrides containing electron-withdrawing or moderately electron-donating groups worked efficiently under these reaction conditions and gave the desired products in 62–79% yields (Scheme 74). However, a strongly electron-donating group like OMe lowered the product yield to 58%. Bromo-substituted symmetrical anhydrides gave lower yields (42–48%) of the desired products due to their poor solubility. Various olefin acceptors reacted smoothly (40–87%) with benzoic anhydrides although the α - or β -substituted olefins gave lower yields for steric or electronic reasons.



Scheme 74 Photocatalytic hydroacylation using carboxylic acid anhydrides.⁷⁴ ^a Reaction time was 24 h

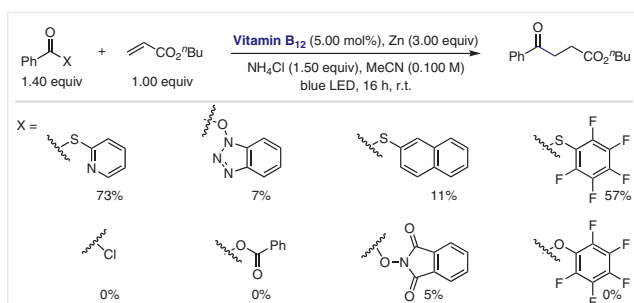
Radical trapping experiments with TEMPO confirmed the formation of an aroyl radical. Stern–Volmer experiments, on the other hand, indicated that a Hantzsch ester is the main quencher of the photoexcited $\text{fac-}^*\text{Ir}(\text{ppy})_3$ at low concentrations. However, the same excited photocatalyst can be quenched by higher concentrations of carboxylic anhydride and $i\text{Pr}_2\text{NEt}$. Based on the above experiments, a plausible mechanism is proposed in Scheme 75 which begins with the photoexcitation of $\text{fac-}^*\text{Ir}(\text{ppy})_3$ with visible light. The photoexcited $\text{fac-}^*\text{Ir}(\text{ppy})_3$ **75.2** undergoes single-electron transfer with the Hantzsch ester ($E_{1/2}^{\text{red}} = +0.887$ V vs SCE)⁷⁵ or $i\text{Pr}_2\text{NEt}$ forming Ir^{II} species **75.3** and the Hantzsch ester (HEH) or $i\text{Pr}_2\text{NEt}$ radical cation (**75.5** or **75.4**). Anhydride **75.6** is reduced by **75.3** ($E_{1/2}^{\text{III/II}} = -2.19$ V vs SCE in MeCN), then fragments to provide the aroyl radical **75.7** which reacts with alkene **75.8** to form α -carbonyl

radical **75.9**. The α -carbonyl radical **75.9** abstracts a hydrogen atom from **75.4**, **74.5**, or Hantzsch ester (**75.5**) to deliver the desired product **75.10**.



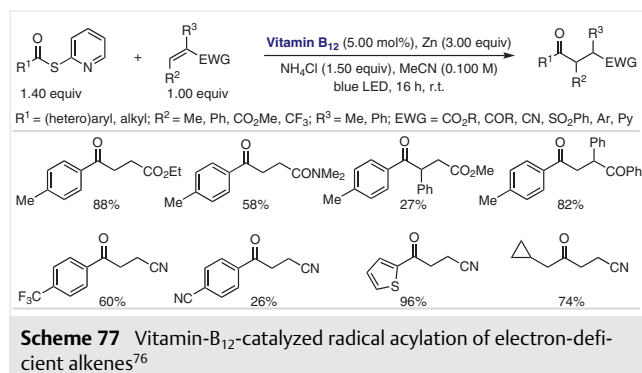
7 Acyl Thioesters as a Source of Acyl Radicals

In 2017, Gryko et al. reported the visible-light driven vitamin-B₁₂-catalyzed generation of an acyl radical from 2-S-pyridyl thioesters (acyl-X reagent) via a single-electron reduction and the subsequent reaction of an acyl radical with electron-deficient olefins.⁷⁶ Scheme 76 demonstrates the superiority of pyridyl thioesters compared to other acylating reagents employed in this reaction. The higher activity of thioesters compared with active esters results from the stronger electrophilic character of the carbonyl group in the thioester derivatives.

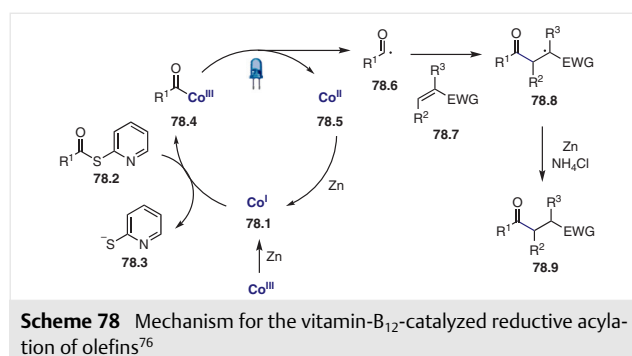


Olefins bearing electron-withdrawing groups such as esters, nitriles, sulfones, amides or ketones all produced the desired ketones in 58–99% yields (Scheme 77). While α -substituted olefins afforded the desired products in good (62–82%) yields, β -substituted olefins gave lower yields (27–47%), probably for steric reasons. Aryl, heteroaryl, and alkyl thioesters reacted equally well under the reaction conditions and formed the desired products in 62–97% yields. In the case of aryl thioesters containing strongly

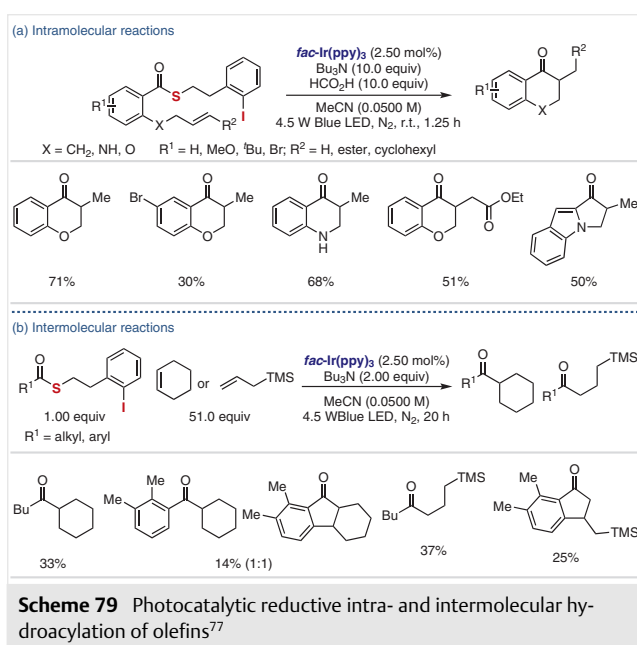
electron-withdrawing groups such as CN or CF₃, the desired products were obtained in lower yields (26–60%), presumably due to their higher susceptibility to reduction (for the compound with a Me substituent: $E_{\text{pc}} = -1.77$ V, CF₃: $E_{\text{pc}} = -1.49$ V, CN: $E_{\text{pc}} = -1.36$ V vs Ag/AgCl).⁷⁶



LCMS detection of the reaction aliquot showed the presence of the acyl-cobalt complex **78.4** in the medium and TEMPO trapping experiments indicated the acyl radical formation. In the absence of the reducing agent zinc, no reaction was observed using Co^{III}- or Co^{II}-vitamin B₁₂, which confirms the formation of an acyl-cobalt complex by the reaction of Co^I-vitamin B₁₂ generated in situ with thioesters. Addition of ND₄Cl in place of NH₄Cl showed deuterium incorporation at the α -position relative to the electron-withdrawing group, indicating the role of NH₄Cl as a proton source during the final step of the reaction. Light ON/OFF experiments support the formation of an acyl radical under constant irradiation of light. The proposed mechanism starts with the reduction of the thioester by Co^I-vitamin B₁₂ (**78.1**) and the generation of acyl-cobalt complex **78.4** which provides the acyl radical **78.6** under irradiation with visible light (Scheme 78). Subsequent addition of the nucleophilic acyl radical to activated olefin **78.7** generates **78.8**, which is reduced by Zn and protonated by NH₄Cl to deliver the desired product **78.9**. The Co^{II}-vitamin B₁₂ catalyst is reduced to Co^I-vitamin B₁₂ by Zn to complete the catalytic cycle.

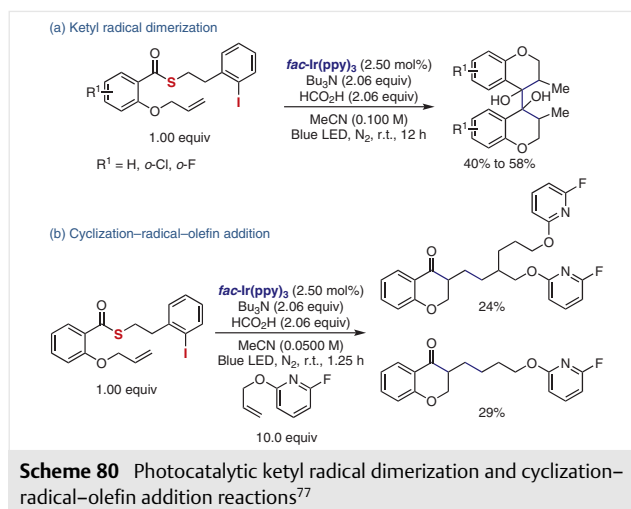


In 2018, McErlean et al. used a thioester as the acyl radical precursor for the hydroacylation of olefins under photocatalytic conditions (Scheme 79).⁷⁷ With 10 equivalents of tributylamine and formic acid, intramolecular acyl radical-olefin addition occurs to form the desired chromanone and indanone derivatives in 18–71% yields (Scheme 79, a). When 2 equivalents of tributylamine and alkenes such as cyclohexene and allyltrimethylsilane were employed in the absence of formic acid (based on McErlean's Supporting Information), intermolecular coupling reactions took place to afford the desired products in 10–37% yields (Scheme 79, b).

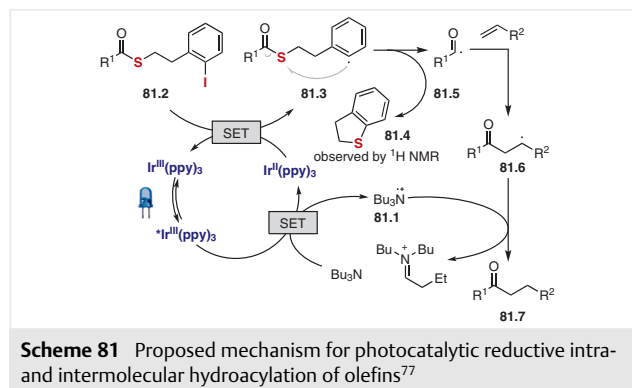


When 2.06 equivalents of tributylamine and formic acid (based on McErlean's Supporting Information) were used, the ketone products were further reduced to form ketyl radicals, which dimerized, forming pinacol-type products (Scheme 80, a). The authors also conducted a one-pot intramolecular cyclization–intermolecular radical–olefin addition reaction, which afforded the two- and three-component coupling products in 29% and 24% yields, respectively (Scheme 80, b).

The unique feature of this reaction is the formation of an acyl radical from the thioester, triggered by the generation of an aryl radical. The idea was inspired by the work of Crich and Yao.⁷⁸ It is proposed that reductive quenching of the excited $^*Ir(ppy)_3$ ($E_{1/2}^{III/II} = +0.31$ V vs SCE)⁵⁶ by tributylamine (triethylamine: $E_{1/2}^{ox} = +0.83$ V vs SCE)⁶¹ produces the tributylamine radical cation **81.1** and $Ir^{II}(ppy)_3$ ($E_{1/2}^{III/II} = -2.19$ V vs SCE) (Scheme 81).⁵⁶ This strongly reducing species reduces the iodobenzene moiety of thioester **81.2** (io-



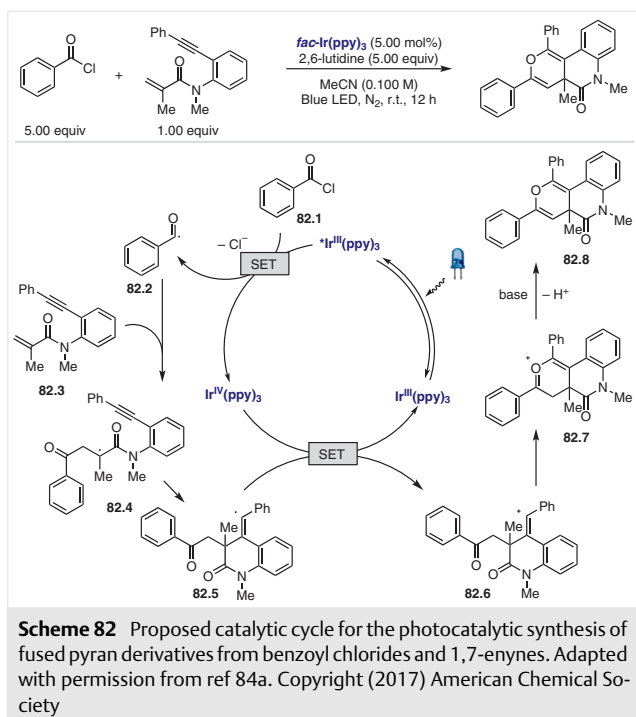
dobenzene: $E_{1/2}^{red} = -1.59$ V vs SCE)⁷⁹ via SET to form the aryl radical **81.3**, which attacks the sulfur to release dihydrobenzothiophene (**81.4**) and an acyl radical **81.5**. Trapping of **81.5** with an olefin forms an alkyl radical intermediate **81.6**, which abstracts a hydrogen atom from tributylamine radical cation **81.1**, liberating the desired product **81.7**.



8 Acyl Chlorides as a Source of Acyl Radicals

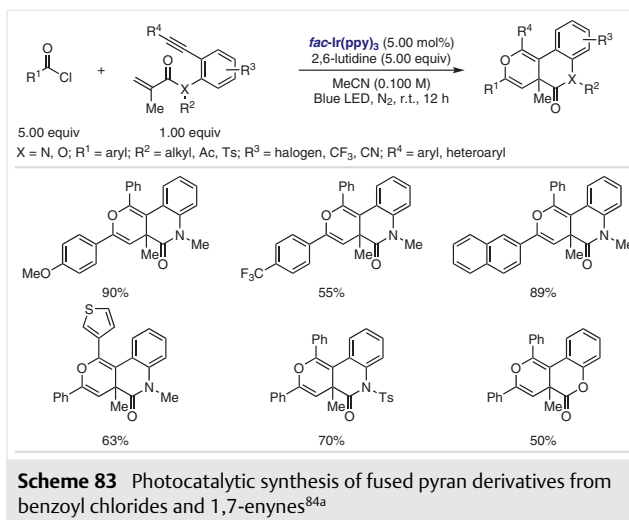
Acyl chlorides are versatile intermediates and have been widely used as electrophilic acylating reagents in organic synthesis. Their electrophilic property can be reversed by a single-electron reduction to generate acyl radicals. An early example of the formation of an acyl radical intermediate from an acyl chloride was reported by van der Kerk et al. in 1957 using triphenyltin hydride.⁸⁰ Under their conditions, triphenyltin chloride and benzaldehyde were formed. A systematic study of the reaction between triphenyltin hydride and benzoyl chloride was conducted by Kuivila in 1960.⁸¹ A mechanism that involved the generation of an acyl radical was further demonstrated by Kuivila in 1966.⁸² The formation of an acyl radical from an acyl chloride via SET with Sml_2 was reported by Kagan et al. in 1981, and the

acyl radical was further reduced to an acyl anion under their reaction conditions.⁸³ Only recently, photoredox catalysis was used for acyl radical formation from acyl chlorides.⁸⁴ In 2017, Xu et al. reported the first protocol to convert a benzoyl chloride into a benzoyl radical, which then reacted with 1,7-enynes to form fused pyran derivatives (Scheme 82).^{84a} The reaction starts with excitation of *fac*-Ir(ppy)₃ by a blue LED and then the excited *fac*-*Ir(ppy)₃ ($E_{1/2}^{\text{IV/III}^*} = -1.73 \text{ V vs SCE}$)⁵⁶ is involved in single-electron reduction of a benzoyl chloride ($E_p = -1.02 \text{ V vs SCE}$)^{84b} forming *fac*-Ir^{IV}(ppy)₃ and benzoyl radical **82.2**. The benzoyl radical then attacks the carbon-carbon double bond of **82.3** to afford an alkyl radical intermediate **82.4**, which undergoes radical cyclization with the alkyne triple bond to form a vinyl radical intermediate **82.5**. Oxidation of the vinyl radical intermediate by *fac*-Ir^{IV}(ppy)₃ gives a vinyl cation species **82.6**. The acyl carbonyl oxygen then attacks the vinyl cation carbon center to form an oxonium ion **82.7**, which is then deprotonated to give the desired product **82.8**.



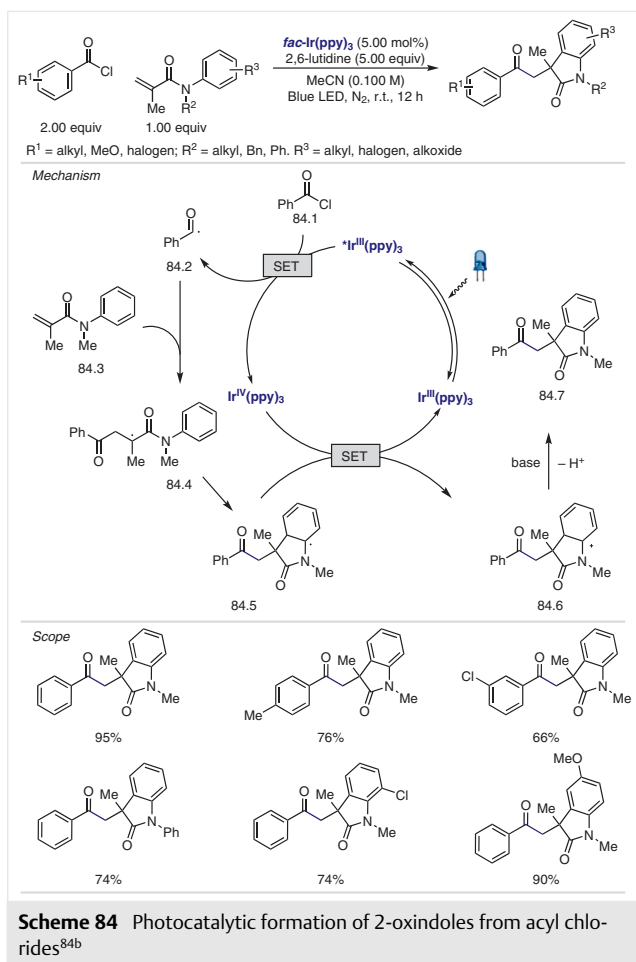
In terms of the acyl chloride substrate scope (Scheme 83), both electron-deficient (e.g., CF₃) and electron-rich (e.g., OMe and Me) substituted benzoyl chlorides coupled to afford the desired products in 55–90% yields. Enyne substrates with alkynyl 3-thiophene and arenes bearing halogen, methyl, and methoxy substituents were tolerated and formed the desired fused pyran derivatives in 63–92% yields (Scheme 83). However, alkynyl alkyl substituents such as *t*-butyl and cyclopropyl groups gave only a trace amount of the desired products. The reaction also tolerates substituents such as Cl, CN, and CF₃ on the arene ring of anilides.

Anilides with different N-protecting groups such as benzyl, acyl, and tosyl were competent, delivering the products in 67–70% yields. Aryl-ester-linked 1,7-enynes were also viable substrates.



In the same year, Xu et al. extended the scope of the reaction to substrates without an alkyne motif (Scheme 84).^{84b} In this reaction, the α -carbonyl radical intermediate **84.4**, generated from the reaction of *N*-phenylmethacrylamide (**84.3**) and the acyl radical **84.2**, undergoes intramolecular cyclization to form intermediate **84.5**, which is oxidized by Ir^{IV} then deprotonated to give a 3,3-dialkyl 2-oxindole derivative. The reaction scope is similar to that described in Xu's previous report (Scheme 83).^{84a}

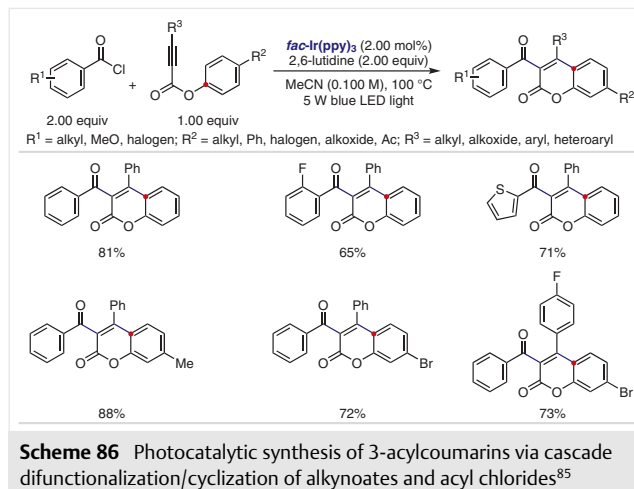
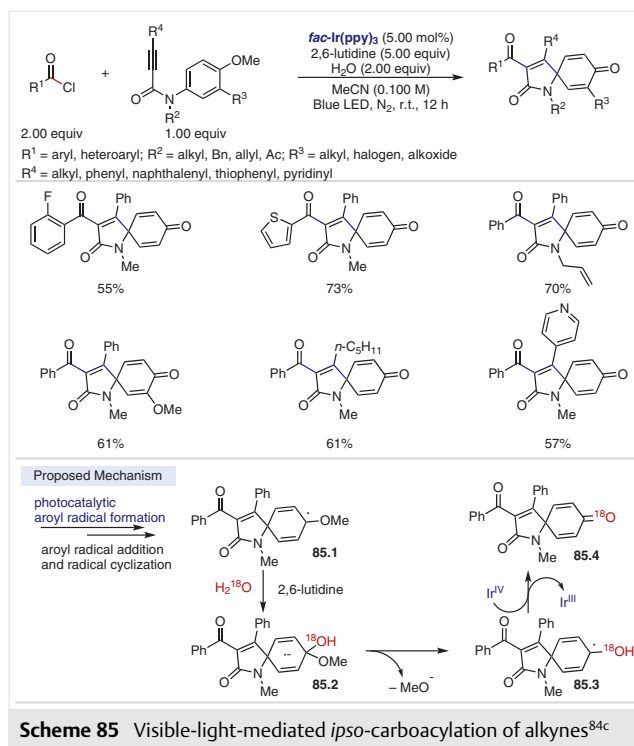
Acyl radicals formed from acyl chlorides can add directly to alkynes. In 2017, Tang et al. synthesized a diverse group of 3-acylspirotrienones via *ipso*-carboacylation of *N*-(*p*-methoxy aryl)propiolamides with acyl chlorides.^{84c} The *p*-methoxy group on the arene ring is critical to formation of the desired products. The reaction conditions worked well with benzoyl chlorides bearing alkyl, methoxy, and halogen substituents and thiophenecarbonyl chloride, affording the desired products in 60–86% yields (Scheme 85). *N*-(*p*-Methoxyaryl)propiolamides containing a benzyl, 2-iodobenzyl acyl or allylic groups on the nitrogen atom were tolerated, providing the 3-acylspirotrienones in 69–73% yields. In terms of the alkynyl substituents (R⁴), pentyl, thiophene, pyridine, naphthalene, and arenes bearing alkyl, methoxy, acyl, CF₃, or halogen groups were compatible and afforded the desired products in 57–88% yields. Mechanistically, the authors proposed that after the initial photocatalytic acyl radical formation followed by a two-step tandem acyl radical-alkyne coupling and radical cyclization, a cyclic radical species **85.1** is generated. An ¹⁸O-labeling experiment suggests that **85.1** is attacked by an exogenous H₂O molecule with assistance from 2,6-lutidine to give a radical



anion intermediate **85.2**. Removal of the methoxy group gives **85.3**, which is then oxidized by Ir^{IV} to afford the desired product **85.4** (Scheme 85).

In 2018, Tang et al. further expanded this type of acyl radical chemistry to the synthesis of 3-acylcoumarins (Scheme 86).⁸⁵ Although thiophenecarbonyl chloride and benzoyl chlorides bearing methyl, methoxy, and halogen substituents were well tolerated, alkyl, vinyl, and electron-deficient (e.g., *p*-O₂NC₆H₄) acyl chlorides failed to produce the desired products. Aryl 3-phenylpropiolates possessing methyl, halogen, methoxy, Ac and CF₃ groups at the *p*-position of the phenoxy ring underwent the reaction smoothly, affording the products in 68% to 80% yields. With respect to the scope of alkynyl substituents, arenes bearing electron-donating and electron-withdrawing groups were compatible under the reaction conditions.

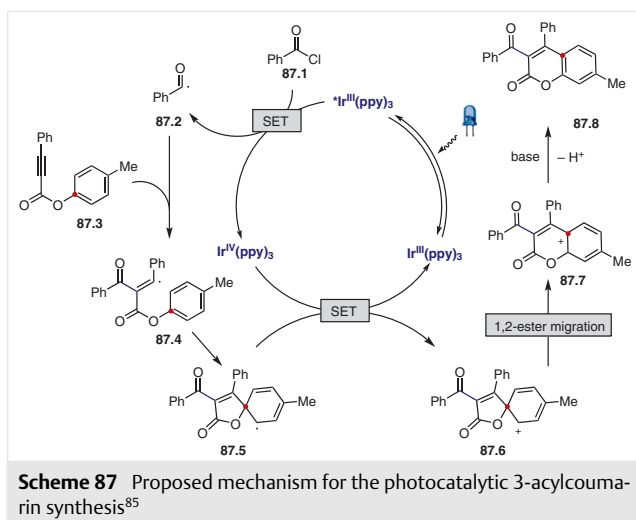
The proposed reaction mechanism is depicted in Scheme 87. Once the radical intermediate **87.4** is formed, it undergoes an intramolecular 5-*exo-trig* cyclization followed by oxidation, giving the cationic species **87.6**. 1,2-Ester migration leads to **87.7**, which upon deprotonation affords the desired product **87.8**. Notably, both Tang's⁸⁵ and



Itoh's³⁶ (Scheme 22) methods involve the formation of a 5-*exo-trig* cyclic intermediate, which is distinct from the transition-metal-catalyzed acyl radical addition reported by Wu⁸⁶ and Wang⁸⁷ in which a 6-*endo-trig* cyclization process was proposed.

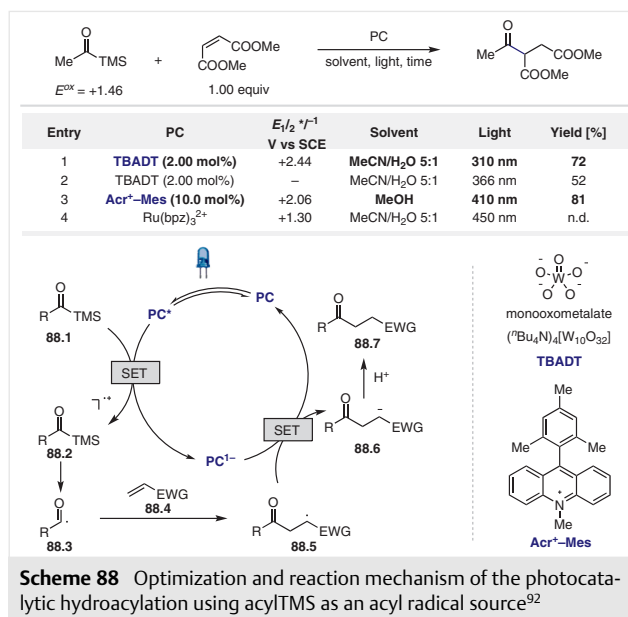
9 Acyl Silanes as a Source of Acyl Radicals

The first isolation of acyl silanes was reported by Brook in 1957.⁸⁸ Acyl silanes are often regarded as unusual carbonyl compounds as a result of the unique feature of an sp²

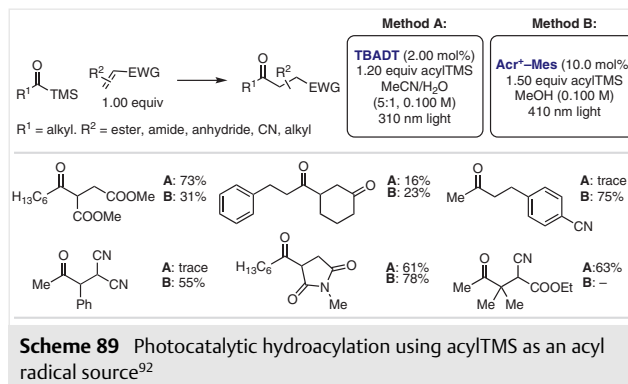


carbon that is bonded to both a silicon and oxygen atom.⁸⁹ In 1969, Brook and Duff reported that photolysis of acyl silanes led to the formation of acyl radical intermediates via Norrish type I cleavage of the acyl-silicon bond.⁹⁰ Electrochemical oxidation of acyl silanes leading to the formation of acyl radicals was described extensively by Keiji and Yoshida between 1986 and 1992.⁹¹ Application of acyl silanes in the formation of acyl radicals under photocatalytic conditions was described by Fagnoni et al. in 2017 (Scheme 88).⁹² Acyl- and benzoyltrimethylsilanes (acylTMS and benzoylTMS) have higher oxidation potentials ($E_{1/2}^{\text{ox}} = +1.26$ to $+1.51$ V vs SCE)⁹² than most of the common transition-metal photocatalysts such as *fac*-Ir(ppy)₃ ($E_{1/2}^{\text{III/II}} = +0.31$ V vs SCE)⁵⁶ and Ru(bpy)₃²⁺ ($E_{1/2}^{\text{II*/I}} = +0.77$ V vs SCE).⁹³ Thus, photocatalysts with stronger oxidizing power are needed to oxidize acylTMSs to acyl radicals. Fagnoni et al. discovered that photoexcited tetrabutylammonium decatungstate (TBADT)⁹⁴ and 9-mesityl-10-methylacridinium tetrafluoroborate (Acr⁺-Mes)⁹⁵ (Scheme 88) could be used to enable the acylation of electron-deficient alkenes. The authors proposed that the excited photocatalyst oxidizes an acylTMS (**88.1**) to an acylTMS radical cation **88.2**, which then loses the TMS group to form a nucleophilic acyl radical **88.3**. The formation of the acyl radical was supported by their TEMPO trap experiments. The alkyl radical intermediate **88.5** formed by the addition of the acyl radical to alkene **88.4** accepts an electron from the reduced photocatalyst to give a carbon anion **88.6**, which is then protonated to form the final product **88.7**.

Regeneration of the TBADT catalyst through oxidation by the carbon radical intermediate was reported by Fagnoni.⁹⁶ Although the absorption spectrum of TBADT is not in the visible light region, it overlaps with the spectrum of sunlight, supporting this catalyst's capacity as a 'window-ledge' catalyst. For the Acr⁺-Mes-catalyzed reaction, *Acr⁺-Mes oxidizes the acylTMS to form an acyl radical and Acr⁺-



Mes ($E_{1/2}^{\text{red}} = -0.57$ V vs SCE), the reduction potential of which is within reach of that of the carbon radical intermediate **88.5** ($E_{1/2}^{\text{red}} \approx -0.63$ V vs SCE). The photocatalytic conditions operate under a different wavelength of light, making it suitable for a range of alkene substrates such as dimethyl maleate, electron-poor styrenes and acrylonitrile (Scheme 89).



10 Conclusions and Future Outlook

Photoredox catalysis has emerged as a powerful tool in organic synthesis and has revolutionized how chemists tackle difficult bond-forming challenges. In this review, we have provided an overview of the development of acyl radical chemistry under photocatalytic conditions. The unique reactivity of photoredox catalysts offers unprecedentedly mild reaction conditions for the generation of versatile acyl radicals from a wide range of precursors including aldehydes, α -ketocarboxylic acids, carboxylic acids and anhy-

drides, acyl thioesters, acyl chlorides, and acyl silanes. The mild conditions also enable the reactions of acyl radicals with a diverse set of coupling partners to construct molecular architectures that are otherwise difficult to prepare. Since the use of photoredox catalysis in acyl radical chemistry only began in 2013 and is still in its infancy, we anticipate that more innovative transformations involving acyl radical intermediates will continue to emerge in the near future.

Funding Information

We thank the National Institute of General Medical Sciences (R35GM119652) for supporting our research.

References

- (1) Caronna, T.; Fronza, G.; Minisci, F.; Porta, O.; Gardini, G. P. *J. Chem. Soc., Perkin Trans. 2* **1972**, 1477.
- (2) (a) Bugaut, X.; Glorius, F. *Chem. Soc. Rev.* **2012**, *41*, 3511. (b) Enders, D.; Niemeier, O.; Henseler, A. *Chem. Rev.* **2007**, *107*, 5606. (c) Stetter, H.; Kuhlmann, H. *Org. React.* **2004**, *40*, 407.
- (3) Duncton, M. A. *J. Med. Chem. Commun.* **2011**, *2*, 1135.
- (4) (a) Boger, D. L.; Mathvink, R. J. *J. Org. Chem.* **1992**, *57*, 1429. (b) Chatgililoglu, C.; Crich, D.; Komatsu, M.; Ryu, I. *Chem. Rev.* **1999**, *99*, 1991.
- (5) (a) Liu, W.; Li, Y.; Liu, K.; Li, Z. *J. Am. Chem. Soc.* **2011**, *133*, 10756. (b) Benati, L.; Calestani, G.; Leardini, R.; Minozzi, M.; Nanni, D.; Spagnolo, P.; Strazzari, S. *Org. Lett.* **2003**, *5*, 1313. (c) Bath, S.; Laso, N. M.; Lopez-Ruiz, H.; Quiclet-Sire, B.; Zard, S. *Z. Chem. Commun.* **2003**, 204.
- (6) Boger, D. L.; Mathvink, R. J. *J. Org. Chem.* **1989**, *54*, 1777.
- (7) (a) Chen, C.; Crich, D.; Papadatos, A. *J. Am. Chem. Soc.* **1992**, *114*, 8313. (b) Crich, D.; Chen, C.; Hwang, J.-T.; Yuan, H.; Papadatos, A.; Walter, R. I. *J. Am. Chem. Soc.* **1994**, *116*, 8937.
- (8) (a) Colley, C. S.; Grills, D. C.; Besley, N. A.; Jockusch, S.; Matousek, P.; Parker, A. W.; Towrie, M.; Turro, N. J.; Gill, P. M. W.; George, M. W. *J. Am. Chem. Soc.* **2002**, *124*, 14952. (b) Hristova, D.; Gatlik, I.; Rist, G.; Dietliker, K.; Wolf, J.-P.; Birbaum, J.-L.; Savitsky, A.; Moebius, K.; Gescheidt, G. *Macromolecules* **2005**, *38*, 7714. (c) Sluggett, G. W.; Turro, C.; George, M. W.; Koptuyug, I. V.; Turro, N. J. *J. Am. Chem. Soc.* **1995**, *117*, 5148.
- (9) Yagci, Y.; Pappas, S. P.; Schnabel, W. Z. *Naturforsch., A: Phys. Sci.* **1987**, *42*, 1425.
- (10) (a) Brown, C. E.; Neville, A. G.; Rayner, D. M.; Ingold, K. U.; Luszyk, J. *Aust. J. Chem.* **1995**, *48*, 363. (b) McGimpsey, W. G.; Scaiano, J. C. *J. Am. Chem. Soc.* **1987**, *109*, 2179. (c) Neville, A. G.; Brown, C. E.; Rayner, D. M.; Luszyk, J.; Ingold, K. U. *J. Am. Chem. Soc.* **1991**, *113*, 1869. (d) Davies, A. G.; Sutcliffe, R. J. *Chem. Soc., Perkin Trans. 2* **1980**, 819.
- (11) (a) Rosenthal, I.; Mossoba, M. M.; Riesz, P. *Can. J. Chem.* **1982**, *60*, 1486. (b) Miranda, M. A.; Galindo, F. *Photo-Fries Reaction and Related Processes*, In *CRC Handbook of Organic Photochemistry and Photobiology*; Horspool, W.; Lenci, F., Ed.; CRC Press: Boca Raton, **2004**, 42–1.
- (12) (a) Coveney, D. J.; Patel, V. F.; Pattenden, G. *Tetrahedron Lett.* **1987**, *28*, 5949. (b) Coveney, D. J.; Patel, V. F.; Pattenden, G.; Thompson, D. M. *J. Chem. Soc., Perkin Trans. 1* **1990**, 2721.
- (13) (a) Wang, H.; Guo, L.-N.; Duan, X.-H. *Adv. Synth. Catal.* **2013**, *355*, 2222. (b) Chaubey, N. R.; Singh, K. N. *Tetrahedron Lett.* **2017**, *58*, 2347. (c) Meng, M.; Wang, G.; Yang, L.; Cheng, K.; Qi, C. *Adv. Synth. Catal.* **2018**, *360*, 1218.
- (14) Wu, X.-F. *Chem. Eur. J.* **2015**, *21*, 12252.
- (15) (a) Prier, C. K.; Rankic, D. A.; MacMillan, D. W. C. *Chem. Rev.* **2013**, *113*, 5322. (b) Skubi, K. L.; Blum, T. R.; Yoon, T. P. *Chem. Rev.* **2016**, *116*, 10035. (c) Shaw, M. H.; Twilton, J.; MacMillan, D. W. C. *J. Org. Chem.* **2016**, *81*, 6898. (d) Romero, N. A.; Nicewicz, D. A. *Chem. Rev.* **2016**, *116*, 10075. (e) Karkas, M. D.; Porco, J. A.; Stephenson, C. R. J. *Chem. Rev.* **2016**, *116*, 9683. (f) Douglas, J. J.; Sevrin, M. J.; Stephenson, C. R. J. *Org. Process Res. Dev.* **2016**, *20*, 1134. (g) Twilton, J.; Le, C.; Zhang, P.; Shaw, M. H.; Evans, R. W.; MacMillan, D. W. C. *Nat. Rev. Chem.* **2017**, *1*, 0052.
- (16) Xiao, W.-J.; Zhou, Q.-Q.; Zou, Y.-Q.; Lu, L.-Q. *Angew. Chem. Int. Ed.* **2018**, in press; DOI: 10.1002/anie.201803102.
- (17) Luca, C.; Davide, R. *Eur. J. Org. Chem.* **2017**, 2056.
- (18) Shi, Z.; Glorius, F. *Chem. Sci.* **2013**, *4*, 829.
- (19) Jhuang, H.-S.; Reddy, D. M.; Chen, T.-H.; Lee, C.-F. *Asian J. Org. Chem.* **2016**, *5*, 1452.
- (20) Jeffrey, J. L.; Terrett, J. A.; MacMillan, D. W. C. *Science* **2015**, *349*, 1532.
- (21) Fan, X. Z.; Rong, J. W.; Wu, H. L.; Zhou, Q.; Deng, H. P.; Tan, J. D.; Xue, C. W.; Wu, L. Z.; Tao, H. R.; Wu, J. *Angew. Chem. Int. Ed.* **2018**, *57*, 8514.
- (22) (a) Shum, L. G.; Benson, S. W. *Int. J. Chem. Kinet.* **1983**, *15*, 433. (b) Simoes, J. M.; Griller, D. *Chem. Phys. Lett.* **1989**, *158*, 175. (c) Berkowitz, J.; Ellison, G. B.; Gutman, D. *J. Phys. Chem.* **1994**, *98*, 2744. (d) Bordwell, F. G.; Satish, A. *J. Am. Chem. Soc.* **1994**, *116*, 8885. (e) Bordwell, F. G.; Liu, W.-Z. *J. Am. Chem. Soc.* **1996**, *118*, 10819. (f) Lund, H.; Daasbjerg, K.; Ochiellini, D.; Pedersen, S. *Russian Journal of Electrochemistry* **1995**, *31*, 865–72. (g) Liu, W.-Z.; Bordwell, F. G. *J. Org. Chem.* **1996**, *61*, 4778. (h) Atkinson, R.; Baulch, D.; Cox, R. A.; Hampson, R. F. Jr.; Kerr, J. A.; Rossi, M. J.; Troe, J. *J. Phys. Chem. Ref. Data* **2000**, *29*, 167. (i) Ervin, K. M.; DeTuri, V. F. *J. Phys. Chem. A* **2002**, *106*, 9947. (j) Luo, Y.-R. *Handbook of Bond Dissociation Energies in Organic Compounds*; CRC Press: Boca Raton, **2002**.
- (23) Iqbal, N.; Choi, S.; You, Y.; Cho, E. J. *Tetrahedron Lett.* **2013**, *54*, 6222.
- (24) Teegardin, K.; Day, J. I.; Chan, J.; Weaver, J. *Org. Process Res. Dev.* **2016**, *20*, 1156.
- (25) Cheng, P.; Qing, Z.; Liu, S.; Liu, W.; Xie, H.; Zeng, J. *Tetrahedron Lett.* **2014**, *55*, 6647.
- (26) White, H. S.; Bard, A. J. *J. Am. Chem. Soc.* **1982**, *104*, 6891.
- (27) Natascia, T.; Ulrich, N.; Alfons, B.; Jozef, P.; Ive, H. *Chem. Eur. J.* **2010**, *16*, 13226.
- (28) Li, J.; Wang, D. Z. *Org. Lett.* **2015**, *17*, 5260.
- (29) Jung, S.; Kim, J.; Hong, S. *Adv. Synth. Catal.* **2017**, *359*, 3945.
- (30) Iqbal, N.; Cho, E. J. *J. Org. Chem.* **2016**, *81*, 1905.
- (31) Mukherjee, S.; Garza-Sanchez, R. A.; Tlahuext-Aca, A.; Glorius, F. *Angew. Chem. Int. Ed.* **2017**, *56*, 14723.
- (32) Choi, G. J.; Zhu, Q.; Miller, D. C.; Gu, C. J.; Knowles, R. R. *Nature* **2016**, *539*, 268.
- (33) Zhang, X.; MacMillan, D. W. C. *J. Am. Chem. Soc.* **2017**, *139*, 11353.
- (34) Shaw, M. H.; Shurtleff, V. W.; Terrett, J. A.; Cuthbertson, J. D.; MacMillan, D. W. C. *Science* **2016**, *352*, 1304.
- (35) Vu, M. D.; Das, M.; Liu, X. W. *Chem. Eur. J.* **2017**, *23*, 15899.
- (36) Kawaai, K.; Yamaguchi, T.; Yamaguchi, E.; Endo, S.; Tada, N.; Ikari, A.; Itoh, A. *J. Org. Chem.* **2018**, *83*, 1988.

- (37) Allen, N. S.; Hurley, J. P.; Bannister, D.; Follows, G. W.; Navaratnam, S.; Parsons, B. J. *J. Photochem. Photobiol., A* **1992**, *68*, 213.
- (38) Majek, M.; Filace, F.; von Wangelin, A. J. *Beilstein J. Org. Chem.* **2014**, *10*, 981.
- (39) We used benzaldehyde as the hydrogen donor to illustrate the mechanism.
- (40) de Souza, G. F.; Bonacin, J. A.; Salles, A. G. Jr. *J. Org. Chem.* **2018**, *83*, 8331.
- (41) Furman, O. S.; Teel, A. L.; Watts, R. J. *Environ. Sci. Technol.* **2010**, *44*, 6423.
- (42) (a) Tanielian, C.; Mechin, R. *J. Photochem. Photobiol., A* **1997**, *107*, 291. (b) Erickson, P. R.; Walpen, N.; Guerard, J. J.; Eustis, S. N.; Arey, J. S.; McNeill, K. *J. Phys. Chem. A* **2015**, *119*, 3233.
- (43) Liu, J.; Liu, Q.; Yi, H.; Qin, C.; Bai, R.; Qi, X.; Lan, Y.; Lei, A. *Angew. Chem. Int. Ed.* **2014**, *53*, 502.
- (44) Young, R. C.; Meyer, T. J.; Whitten, D. G. *J. Am. Chem. Soc.* **1976**, *98*, 286.
- (45) Chu, L.; Lipshultz, J. M.; MacMillan, D. W. C. *Angew. Chem. Int. Ed.* **2015**, *54*, 7929.
- (46) Lowry, M. S.; Goldsmith, J. I.; Slinker, J. D.; Rohl, R.; Pascal, R. A.; Malliaras, G. G.; Bernhard, S. *Chem. Mater.* **2005**, *17*, 5712.
- (47) (a) Tsuji, J.; Yamada, T.; Minami, I.; Yuhara, M.; Nisar, M.; Shimizu, I. *J. Org. Chem.* **1987**, *52*, 2988. (b) Gooßen, L. J.; Zimmermann, B.; Knauber, T. *Angew. Chem. Int. Ed.* **2008**, *47*, 7103. (c) Shang, R.; Yang, Z.-W.; Wang, Y.; Zhang, S.-L.; Liu, L. *J. Am. Chem. Soc.* **2010**, *132*, 14391. (d) Weaver, J. D.; Ka, B. J.; Morris, D. K.; Thompson, W.; Tunge, J. A. *J. Am. Chem. Soc.* **2010**, *132*, 12179. (e) Gooßen, L. J.; Lange, P. P.; Rodriguez, N.; Linder, C. *Chem. Eur. J.* **2010**, *16*, 3906. (f) Wang, C.; Rakshit, S.; Glorius, F. *J. Am. Chem. Soc.* **2010**, *132*, 14006. (g) Shang, R.; Ji, D.-S.; Chu, L.; Fu, Y.; Liu, L. *Angew. Chem. Int. Ed.* **2011**, *50*, 4470. (h) Hu, P.; Zhang, M.; Jie, X.; Su, W. *Angew. Chem. Int. Ed.* **2012**, *51*, 227. (i) Fromm, A.; van Wuelen, C.; Hackenberger, D.; Gooßen, L. J. *J. Am. Chem. Soc.* **2014**, *136*, 10007.
- (48) Gooßen, L. J.; Rudolphi, F.; Ooppel, C.; Rodriguez, N. *Angew. Chem. Int. Ed.* **2008**, *47*, 3043.
- (49) Cheng, W.-M.; Shang, R.; Yu, H.-Z.; Fu, Y. *Chem. Eur. J.* **2015**, *21*, 13191.
- (50) Zhou, C.; Li, P.; Zhu, X.; Wang, L. *Org. Lett.* **2015**, *17*, 6198.
- (51) Xu, N.; Li, P.; Xie, Z.; Wang, L. *Chem. Eur. J.* **2016**, *22*, 2236.
- (52) Wang, G.-Z.; Shang, R.; Cheng, W.-M.; Fu, Y. *Org. Lett.* **2015**, *17*, 4830.
- (53) Zhang, M.; Xi, J.; Ruzi, R.; Li, N.; Wu, Z.; Li, W.; Zhu, C. *J. Org. Chem.* **2017**, *82*, 9305.
- (54) (a) Jamison, C. R.; Overman, L. E. *Acc. Chem. Res.* **2016**, *49*, 1578. (b) Slutskyy, Y.; Overman, L. E. *Org. Lett.* **2016**, *18*, 2564.
- (55) Petersen, W. F.; Taylor, R. J. K.; Donald, J. R. *Org. Lett.* **2017**, *19*, 874.
- (56) Flamigni, L.; Barbieri, A.; Sabatini, C.; Ventura, B.; Barigelletti, F. *Top. Curr. Chem.* **2007**, *281*, 143.
- (57) Bai, Q.-F.; Jin, C.; He, J.-Y.; Feng, G. *Org. Lett.* **2018**, *20*, 2172.
- (58) Huang, H.; Zhang, G.; Chen, Y. *Angew. Chem. Int. Ed.* **2015**, *54*, 7872.
- (59) Tan, H.; Li, H.; Ji, W.; Wang, L. *Angew. Chem. Int. Ed.* **2015**, *54*, 8374.
- (60) Ji, W.; Tan, H.; Wang, M.; Li, P.; Wang, L. *Chem. Commun.* **2016**, *52*, 1462.
- (61) Roth, H. G.; Romero, N. A.; Nicewicz, D. A. *Synlett* **2016**, *27*, 714.
- (62) Bergonzini, G.; Cassani, C.; Wallentin, C.-J. *Angew. Chem. Int. Ed.* **2015**, *54*, 14066.
- (63) Zhou, Q.-Q.; Guo, W.; Ding, W.; Wu, X.; Chen, X.; Lu, L.-Q.; Xiao, W.-J. *Angew. Chem. Int. Ed.* **2015**, *54*, 11196.
- (64) Candish, L.; Freitag, M.; Gensch, T.; Glorius, F. *Chem. Sci.* **2017**, *8*, 3618.
- (65) Chateaufneuf, J.; Luszyk, J.; Ingold, K. U. *J. Am. Chem. Soc.* **1988**, *110*, 2886.
- (66) Pettersson, F.; Bergonzini, G.; Cassani, C.; Wallentin, C.-J. *Chem. Eur. J.* **2017**, *23*, 7444.
- (67) Zhang, M.; Ruzi, R.; Xi, J.; Li, N.; Wu, Z.; Li, W.; Yu, S.; Zhu, C. *Org. Lett.* **2017**, *19*, 3430.
- (68) Zhang, M.; Li, N.; Tao, X.; Ruzi, R.; Yu, S.; Zhu, C. *Chem. Commun.* **2017**, *53*, 10228.
- (69) Ruzi, R.; Zhang, M.; Ablajan, K.; Zhu, C. *J. Org. Chem.* **2017**, *82*, 12834.
- (70) Zhang, M.; Xie, J.; Zhu, C. *Nat. Commun.* **2018**, *9*, 3517.
- (71) Pandey, G.; Pooranchand, D.; Bhalerao, U. T. *Tetrahedron* **1991**, *47*, 1745.
- (72) Stache, E. E.; Ertel, A. B.; Rovis, T.; Doyle, A. G. *ACS Catal.* **2018**, *8*, 11134.
- (73) Bergonzini, G.; Cassani, C.; Lorimer-Olsson, H.; Hoerberg, J.; Wallentin, C.-J. *Chem. Eur. J.* **2016**, *22*, 3292.
- (74) Dong, S.; Wu, G.; Yuan, X.; Zou, C.; Ye, J. *Org. Chem. Front.* **2017**, *4*, 2230.
- (75) Zhu, X.-Q.; Li, H.-R.; Li, Q.; Ai, T.; Lu, J.-Y.; Yang, Y.; Cheng, J.-P. *Chem. Eur. J.* **2003**, *9*, 871.
- (76) Ociepa, M.; Baka, O.; Narodowicz, J.; Gryko, D. *Adv. Synth. Catal.* **2017**, *359*, 3560.
- (77) Norman, A. R.; Yousef, M. N.; McErlean, C. *Org. Chem. Front.* **2018**, *5*, 3267.
- (78) Crich, D.; Yao, Q. *J. Org. Chem.* **1996**, *61*, 3566.
- (79) Fry, A. J.; Krieger, R. L. *J. Org. Chem.* **1976**, *41*, 54.
- (80) van der Kerk, G. J. M.; Noltes, J. G.; Luijten, J. G. A. *J. Appl. Chem.* **1957**, *7*, 356.
- (81) Kuivila, H. G. *J. Org. Chem.* **1960**, *25*, 284.
- (82) Kuivila, H. G.; Walsh, E. J. *J. Am. Chem. Soc.* **1966**, *88*, 571.
- (83) (a) Girard, P.; Couffignal, R.; Kagan, H. B. *Tetrahedron Lett.* **1981**, *22*, 3959. (b) Souppe, J.; Namy, J. L.; Kagan, H. B. *Tetrahedron Lett.* **1984**, *25*, 2869.
- (84) (a) Li, C.-G.; Xu, G.-Q.; Xu, P.-F. *Org. Lett.* **2017**, *19*, 512. (b) Xu, S.-M.; Chen, J.-Q.; Liu, D.; Bao, Y.; Liang, Y.-M.; Xu, P.-F. *Org. Chem. Front.* **2017**, *4*, 1331. (c) Liu, Y.; Wang, Q.-L.; Zhou, C.-S.; Xiong, B.-Q.; Zhang, P.-L.; Yang, C.-a.; Tang, K.-W. *J. Org. Chem.* **2018**, *83*, 2210. (d) Wang, C. M.; Song, D.; Xia, P. J.; Wang, J.; Xiang, H. Y.; Yang, H. *Chem. Asian. J.* **2018**, *13*, 271.
- (85) Liu, Y.; Wang, Q.-L.; Zhou, C.-S.; Xiong, B.-Q.; Zhang, P.-L.; Kang, S.-J.; Yang, C.-A.; Tang, K.-W. *Tetrahedron Lett.* **2018**, *59*, 2038.
- (86) Mi, X.; Wang, C.; Huang, M.; Wu, Y.; Wu, Y. *J. Org. Chem.* **2015**, *80*, 148.
- (87) Yan, K.; Yang, D.; Wei, W.; Wang, F.; Shuai, Y.; Li, Q.; Wang, H. *J. Org. Chem.* **2015**, *80*, 1550.
- (88) Brook, A. G. *J. Am. Chem. Soc.* **1957**, *79*, 4373.
- (89) (a) Page, P. C. B.; Klair, S. S.; Rosenthal, S. *Chem. Soc. Rev.* **1990**, *19*, 147. (b) Zhang, H.-J.; Priebbenow, D. L.; Bolm, C. *Chem. Soc. Rev.* **2013**, *42*, 8540.
- (90) (a) Brook, A. G.; Duff, J. M. *J. Am. Chem. Soc.* **1969**, *91*, 2118. (b) Brook, A. G.; Dillon, P. J.; Pearce, R. *Can. J. Chem.* **1971**, *49*, 133.
- (91) (a) Kunio, M.; Shuko, O.; Kyoko, I.; Osamu, K.; Tohru, T.; Keiji, Y. *Chem. Lett.* **1986**, *15*, 805. (b) Yoshida, J.-i.; Matsunaga, S.-i.; Isoe, S. *Tetrahedron Lett.* **1989**, *30*, 5293. (c) Yoshida, J.; Itoh, M.; Matsunaga, S.; Isoe, S. *J. Org. Chem.* **1992**, *57*, 4877.

- (92) Capaldo, L.; Riccardi, R.; Ravelli, D.; Fagnoni, M. *ACS Catal.* **2017**, *8*, 304.
- (93) Rillema, D. P.; Allen, G.; Meyer, T. J.; Conrad, D. *Inorg. Chem.* **1983**, *22*, 1617.
- (94) Waele, V. D.; Poizat, O.; Fagnoni, M.; Bagno, A.; Ravelli, D. *ACS Catal.* **2016**, *6*, 7174.
- (95) Tsudaka, T.; Kotani, H.; Ohkubo, K.; Nakagawa, T.; Tkachenko, N. V.; Lemmetyinen, H.; Fukuzumi, S. *Chem. Eur. J.* **2017**, *23*, 1306.
- (96) Ravelli, D.; Protti, S.; Fagnoni, M. *Acc. Chem. Res.* **2016**, *49*, 2232.